Structural Closure of Einstein–Cartan–Holst Dark Energy: A No-Go Theorem and the Matter-Bounce Tests It Does Not Predict

Houston Golden[1, *]

[1] *Independent Researcher, Los Angeles, California, USA*

(Dated: May 22, 2026 PDT — v1A.0.35)

We establish that the four enumerated minimal-Einstein-Cartan-Holst (ECH) spin-torsion channels for sourcing late-time dark energy fail at the amplitude level. This is a channel-level closure, not an operator-level theorem: the four enumerated routes (NJL, one-loop EA, Immirzi running, parity-CMB) are not proven to be a complete diffeomorphism-invariant operator basis for the minimal-ECH effective action; we acknowledge missing operators (Jackiw-Pi gravitational Chern-Simons $R\wedge\tilde{R}$, parity-odd four-fermion partner with $\gamma_{\rm BI}/(\gamma_{\rm BI}^2+1)\cdot 8\pi G$ coefficient) explicitly in Sec. IV and Sec. XI. Through 7 foundation studies (Foundations A–G) and 6 observational research branches (Branches H, J, L, M, N, O) we report 13 logically-independent mechanism-class constraints (the prior count of 14 retained Barrier 8 as the observational consequence of the perturbation-transparency theorem Barrier 14; merged here under the perturbation-transparency umbrella since they are not logically independent) that collectively constrain the enumerated channels of the minimal-ECH route from the quantum bounce to observable dark energy. The central result is a perturbation-transparency theorem: for canonical scalar matter, torsion vanishes at all perturbation orders, the Holst dual contraction $\epsilon^{\mu\nu\rho\sigma}R_{\mu\nu\rho\sigma}$ vanishes identically by the first Bianchi identity, and the Holst sector decouples from all scalar/tensor perturbation observables (Sec. X). The proposed link from ECH to a late-time vacuum energy requires a phenomenological dimensional ansatz beyond the minimal framework (Appendix B), and is closed by the 13 logically-independent barriers of Sec. IX (14 historical catalog entries, of which B8 is subsumed by B14 per the perturbation-transparency theorem). A structural incompatibility (Sec. XIV D) exists between the dark-energy mechanism, which requires $N_{\rm tot}\approx 92$ post-bounce e-folds, and the matter-bounce $f_{\rm NL}=-35/8$ signature, which would be *definitively* erased at SPHEREx-accessible comoving wavenumbers by that many e-folds (a contracting-phase quantity mode with $k_{\rm SPHEREx}\sim 10^{-1}\,h/$Mpc is pushed to $k^{\rm phys}_{\rm bounce}\sim k^{\rm phys}_{\rm SPHEREx}\,e^{N_{\rm tot}-N_{\rm exit}}\sim e^{32}\,k^{\rm phys}_{\rm SPHEREx}$ at $N_{\rm tot}\sim 92$, $N_{\rm exit}\sim 60$ (the relative e-fold differential between bounce and CMB horizon-exit; comoving wavenumbers k are constant by definition and only physical scales scale with $a^{-1}\propto e^{-N}$), deep inside the inflationary subhorizon regime carrying purely vacuum-inflationary fluctuations rather than matter-bounce contraction modes); ECH is therefore not internally consistent as both a dark-energy generator and a matter-bounce host. The two predictions discussed below as "surviving" are accordingly *not* predictions of ECH itself, but bounce-class and GR+ALP-class observables that the ECH closure does not forbid in the parameter regimes complementary to its dark-energy mechanism; we report them here because they remain testable signatures of any bounce model in the broader programme. Specifically: (i) $f_{\rm NL}=-35/8$ is a property of the *matter-bounce class* [1], derived from the contraction-phase cubic action with no ECH input, testable by SPHEREx at 3–5σ realistic significance (detailed multi-tracer Fisher forecast in Paper II, Ref. [2]); and (ii) spectator-ALP birefringence $\beta\approx 0.27^\circ$ consistent with the published Planck/ACT DR6 3.6σ signal arises in any GR+ALP setup with the same parameters and is *not* derived from the ECH action. The role of this paper is the *channel-level no-go* for the four enumerated minimal-ECH dark-energy routes (Sec. IV) at amplitude-budget granularity; we do not claim a full operator-basis closure of the most general ECH parity-odd / torsion-sourced sector (Jackiw–Pi gravitational Chern–Simons and the parity-odd four-fermion partner of R1 are listed but not separately enumerated in the four routes; their explicit closure is left to a follow-up operator-level analysis). The complementary observational programme is hosted in the bounce-class portfolio (Paper II, Paper I(b)), not in ECH per se. ΛCDM+$\Delta N_{\rm eff}$ MCMC verification, NaMaster pipeline validation, and ALP parameter fitting are documented separately in the companion Paper I(b) [3].

PACS numbers: 98.80.-k, 04.50.Kd, 04.60.Pp, 95.36.+x

CONTENTS

* houston@hubify.com

I. INTRODUCTION

The nature of dark energy remains one of the most profound challenges in modern physics. While the ΛCDM model successfully accounts for observed cosmic acceleration [4], it faces severe theoretical difficulties—most notably the cosmological constant problem [5]. DESI 2024–2025 BAO results suggest dynamical dark energy at 3.1–4.2σ (dataset-dependent) [6, 7], adding urgency to the search for extensions of the standard model.

This work presents and closes a phenomenological framework that connects ECH spin-torsion cosmology

to dark energy. The structural conclusion is a *channel-level amplitude no-go* on the four enumerated minimal-ECH dark-energy routes (Sec. IV): the 14 constraints (Sec. IX, 13 logically-independent with B8 subsumed by B14) close those routes at amplitude-budget granularity. The surviving phenomenological predictors—matter-bounce $f_{\rm NL}$ and spectator-ALP birefringence—are mechanism-independent and shared by other UV completions.

Our approach builds on three theoretical pillars:

1. *Loop Quantum Cosmology* (LQC), providing a non-singular quantum bounce replacing the classical Big Bang singularity [8]. The bounce occurs at $\rho_{\rm crit} \simeq 0.27$–$0.41\,\rho_{\rm Pl}$ (Barbero-Immirzi entropy-counting scheme dependent; Sec. II B).

2. *Einstein-Cartan theory* incorporating fermionic spin-torsion coupling, generating four-fermion contact interactions and preventing gravitational singularities through torsion-induced repulsion at extreme densities [9, 10].

3. *Black hole universe origin*, where a rotating parent black hole spawns a non-singular baby universe through torsion-regulated gravitational collapse [11]. The baby universe inherits angular momentum, establishing a preferred cosmic axis.

A. Theoretical Foundations and Novel Synthesis

Our framework collects well-established theoretical components and tests them as a channel-level amplitude closure of the four enumerated minimal-ECH dark-energy routes (we do not claim a full operator-basis closure; see Sec. IV "Scope" for the explicit operators omitted). The original contributions are:

1. *14-constraint catalog and perturbation-transparency observation*: Through 7 foundation studies (Foundations A–G) and 6 observational research branches (Branches H, J, L, M, N, O), we establish 14 mechanism-class structural constraints (one of which, B8, is the observational consequence of the perturbation-transparency theorem B14 and is retained in the catalog for historical mechanism-class completeness) mapping the minimal ECH parameter space. The central result is that minimal ECH gravity is perturbation-transparent for canonical scalar matter: torsion vanishes at all orders, the Holst sector decouples cleanly from scalar/tensor observables, and tests of γ shift to nonperturbative parity-violating channels (ALP birefringence, primordial GWs).

2. *Structural tension between dark-energy suppression and bounce $f_{\rm NL}$*: We identify an incompatibility between the inflationary-suppression dark-energy mechanism ($N_{\rm tot} \approx 92$ e-folds required) and the matter-bounce $f_{\rm NL} = -35/8$ prediction (*definitively* erased by $N_{\rm tot} \gtrsim 60$ inflationary e-folds at SPHEREx-relevant scales, since the SPHEREx accessible band $k \sim 10^{-4}$–$10^{-1}\,h$/Mpc maps to bounce-era *physical* scales $k^{\rm phys}_{\rm bounce} = k^{\rm phys}_{\rm SPHEREx}\, e^{N_{\rm tot}-N_{\rm exit}}$ at $N_{\rm tot} \sim 92$ and $N_{\rm exit} \sim 60$ (relative e-fold differential ~ 32; comoving k are constant by definition, only physical scales scale with $a^{-1} \propto e^{-N}$) that lie deep inside the inflationary subhorizon regime where the observable bispectrum is dominated by vacuum-inflationary modes rather than the matter-bounce contraction modes; see Sec. XIV D), establishing that these are independent observational programs.

3. *Survival of mechanism-independent tests*: Despite ECH structural closure, two predictions of the broader bounce/ALP landscape survive and are testable by SPHEREx (2028) and LiteBIRD (early 2030s) independently of any specific UV completion.

B. Paper Organization

Section II develops the ECH theoretical framework. Section III presents observational signatures (galaxy spin null, CMB EB). Section IV closes each of the four standard ECH routes (NJL, one-loop EA, Immirzi running, parity-CMB) at the amplitude level. Section V covers the galaxy-spin data methods. Sections VI–VIII provide systematic analysis, falsification criteria, and related work. The core results occupy Secs. IX–XI: the 13 logically-independent structural barriers (14 historical catalog entries), perturbation-transparency observation, and hybrid loophole rejection. Section XII discusses the inflationary suppression factor and theoretical implications. Section XIII summarizes surviving mechanism-independent tests. Section XIV addresses limitations. Section XV concludes.

Companion paper.—ΛCDM+$\Delta N_{\rm eff}$ MCMC verification (Cobaya v3.6.1, 424,781 samples), NaMaster pseudo-C_ℓ pipeline validation, spectator-ALP MCMC parameter fitting, and a cross-paper reproducibility manifest are reported in Paper I(b) [3]. Cosmological parameter values referenced in this paper ($H_0 = 67.68 \pm 1.06$, $\Delta N_{\rm eff} \approx 0$, etc.) are from that companion.

Appendices provide the parameter summary (Appendix A) and dimensional analysis (Appendix B). Supplementary materials are at `https://github.com/Hubify-Projects/bigbounce`.

TABLE I. Executive summary: systematic investigation of bounce-cosmology dark-energy routes within ECH. Structural constraints narrow phenomenological pathways; the surviving testable prediction is the matter-bounce $f_{\rm NL} = -35/8$ [1].

Question	**Result**	**Status**
Can bounce derive dark energy?	14 constraints map minimal-ECH route space	Phen. assumption[a] required.
Is there a nonsingular bounce?	LQC: $\rho_c \simeq 0.27$–$0.41\,\rho_{\rm Pl}$	**Yes** (LQC holonomy).
ECH visible in scalar/tensor pert.?	Perturbation-transparency result	Decouples; tests → ALP/GW.
Testable prediction?	$f_{\rm NL} = -35/8$ (Paper II forecast[b])	**Yes**, class-level[c].
H_0/σ_8 tension resolution?	$H_0 = 67.68 \pm 1.06$, $\Delta N_{\rm eff} \approx 0$	Recovers ΛCDM.

[a]Reparameterized as sensitivity to $N_{\rm tot}$; not solved. [b]3–5σ realistic after full systematic budget (GR-projection, b_ϕ uncertainty, photo-z degradation) under Heinrich+2024 $\sigma(f_{\rm NL})\approx 0.7$. [c]Class-level: scalar-only $w = 0$ matter-bounce under Assumption (f) of Paper II; not fully mechanism-independent across the bouncing-cosmology landscape; not a distinctive ECH prediction. MCMC details in companion Paper I(b) [3].

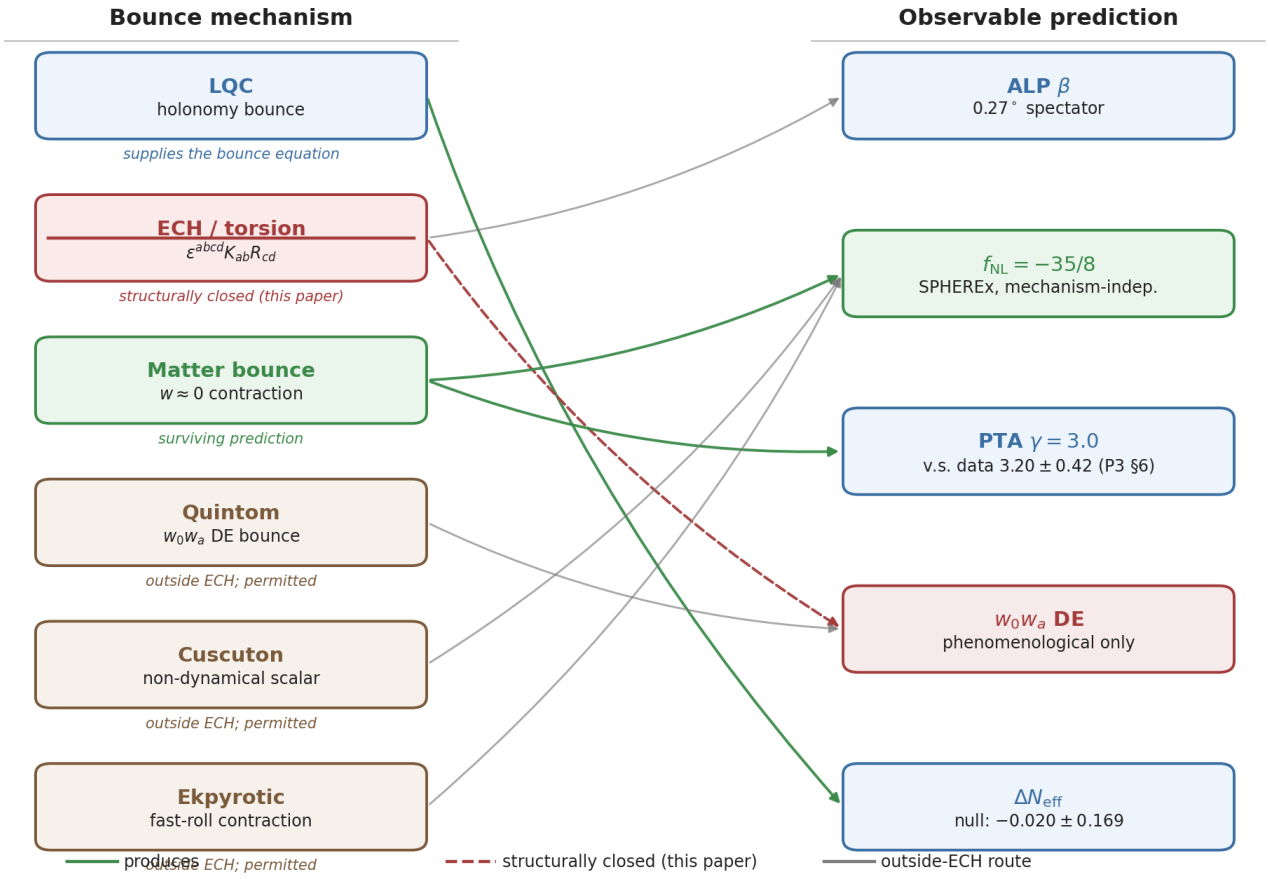

FIG. 1. Bounce-mechanism → observable-prediction map. Left column: candidate non-singular bounce mechanisms (LQC, ECH/torsion, matter bounce, quintom-B, Cuscuton, ekpyrotic). Right column: distinctive observable channels. ECH appears bordered with a dashed box marked *structurally closed (this paper)*—the 14-constraint catalog narrows minimal-ECH dark-energy routes to zero phenomenologically free pathways.

II. THEORETICAL FRAMEWORK

A. Loop Quantum Cosmology and the Holst Action

1. *Einstein-Cartan-Holst Action*

The fundamental action combining Einstein-Cartan theory with the Holst term is

$$S_{\rm ECH} = \frac{1}{16\pi G}\int d^4x\, e\left[e^\mu_a\, e^\nu_b\, R^{ab}{}_{\mu\nu} + \frac{1}{\gamma}\varepsilon^{abcd}\, e_a^{\ \mu}\, e_b^{\ \nu}\, R_{cd\mu\nu} + \frac{1}{4}T^{abc}T_{abc}\right] + S_{\rm matter}, \tag{1}$$

where $e = \det(e^a_\mu)$ is the tetrad determinant, $R^{ab}{}_{\mu\nu}$ is the curvature of the Lorentz connection, γ is the Barbero-Immirzi parameter, and T^{abc} is the torsion tensor. The Holst term contributes non-trivially when fermions are present. This construction builds on Freidel, Minic & Takeuchi [12], who established that the Barbero-Immirzi parameter becomes physically observable through its

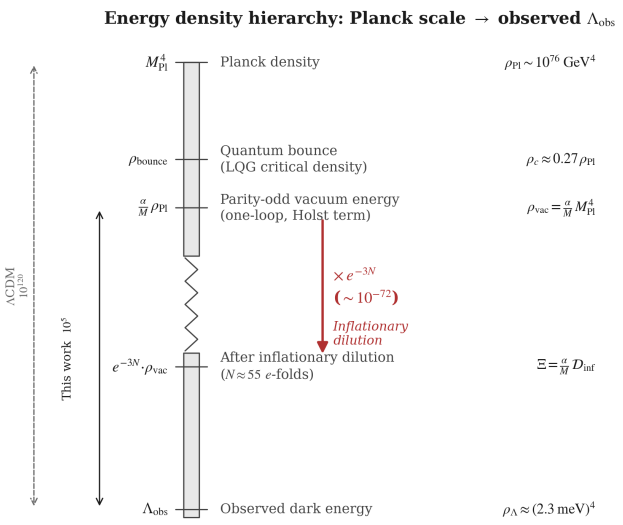

FIG. 2. Energy density hierarchy from the Planck scale to the observed dark energy scale, illustrating the phenomenological scaling ansatz $\rho_{\rm vac} \sim [(\alpha/M)\, M_{\rm Pl}]\, M_{\rm Pl}^4$ (Sec. II A 2, Appendix B). This ansatz is dimensionally correct on-shell at the bounce but is *not* derived from the ECH action.

coupling to fermionic matter. The $T^{abc}T_{abc}$ term in Eq. (1) is a shorthand for the four-fermion contact interaction obtained after integrating out the non-propagating torsion; it is not an independently specified kinetic term.

The Barbero-Immirzi parameter is fixed by LQG black hole entropy:

$$\gamma = 0.274 \pm 0.020, \tag{2}$$

with the ABCK counting [13] giving $\gamma_{\rm ABCK} \approx 0.274$ and DLM full SU(2) counting [14, 15] giving $\gamma_{\rm DLM} \approx 0.2375$.

2. Derivation of the Parity-Odd Term

Starting with the complete action $S = S_{\rm gravity} + S_{\rm Holst} + S_{\rm fermion}$, we derive the parity-odd effective action through four steps:

Step 1: Torsion Activation.—Torsion is determined algebraically by the fermionic spin density:

$$T^{abc} = 8\pi G\, S^{abc}, \tag{3}$$

where $S^{abc} = \frac{1}{4}\bar\psi\gamma^{[a}\gamma^{bc]}\psi$.

Step 2: Four-Fermion Contact Interaction.—Substituting Eq. (3) and integrating out torsion:

$$\mathcal{L}_{\rm int} = -\frac{3\pi G_N}{2} \times \frac{\gamma^2}{\gamma^2+1} \times J^5_\mu\, J^{5\mu}, \tag{4}$$

where $J^{5\mu} = \bar\psi\gamma^\mu\gamma^5\psi$ is the axial current.

Step 3: Parity-Odd Effective Action.—Motivated by the Holst+non-minimal-fermion construction of Mercuri [16] (which shows that the Nieh–Yan invariant is reconstructed and the Barbero–Immirzi parameter drops out of the classical dynamics), we introduce as a phenomenological ansatz the parity-odd term:

$$S_{\rm eff} = \frac{\alpha}{M}\int e_I \wedge e_J \wedge \mathcal{F}^{IJ}[K, \mathring{R}], \tag{5}$$

where $M = M_{\text{area-gap}} \sim M_{\rm Pl}/\sqrt{\gamma}$ is the LQG area-gap (from the LQG area-gap $\Delta \propto \gamma\,\ell_P^2$, the inverse-length / mass scale is $M_\Delta \sim M_{\rm Pl}/\sqrt{\gamma}$ up to numerical constants; v1A.0.28 R7 GPT-m1 closure: prior $M \sim \sqrt{\gamma}\, M_{\rm Pl}$ inverted the scaling) mass scale and α is a dimensionless coupling.

In components, the leading contribution reduces to

$$S_{\rm eff} = \int d^4x\,\sqrt{-g}\,\frac{\alpha}{M}\,\varepsilon^{\mu\nu\rho\sigma}\, e^I_\mu\, e^J_\nu\, \mathcal{F}_{IJ\rho\sigma}, \tag{6}$$

which has naive mass dimension $[\mathcal{L}_{\rm odd}] = +1$—three units short of the required $+4$ (see Appendix B for the full dimensional counting). The identification $\rho_\Lambda = \Xi\, M_{\rm Pl}^4$ is therefore a *scaling ansatz*, not a controlled EFT calculation.

Step 4: Parity-Odd Coefficient.—Following Freidel *et al.* [12] and Shapiro & Teixeira [17], the one-loop estimate is

$$\frac{\alpha}{M} \sim \frac{g^2}{32\pi^2}\,\frac{\gamma}{M}\,\ln\!\left(\frac{\Lambda_{\rm UV}^2}{\mu^2}\right) + \delta_{\rm NY}, \tag{7}$$

motivating the order of magnitude $[(\alpha/M)\, M_{\rm Pl}] \sim 10^{-2}$. We treat α/M as a phenomenological parameter constrained by data.

3. Parameter Naturalness

The parent black hole mass must exceed $M_{\rm crit} \approx 10^{-3} M_\odot$, easily satisfied by any astrophysical black hole. Required dilution of inherited rotation is naturally achieved through ~ 50 e-folds of inflation.

B. Black Hole Interior and Quantum Bounce

In Loop Quantum Cosmology, holonomy corrections produce a non-singular bounce at Planck-scale densities [8]:

$$H^2 = \frac{8\pi G}{3}\,\rho\left[1 - \frac{\rho}{\rho_{\rm crit}}\right], \tag{8}$$

$$\rho_{\rm crit} = \frac{3}{8\pi G\,\gamma^2\,\Delta} = \frac{\sqrt{3}}{32\pi^2\gamma^3}\,\rho_{\rm Pl} \simeq 0.27\,\rho_{\rm Pl}, \tag{9}$$

with $\Delta = 4\sqrt{3}\pi\gamma\,\ell_P^2$ the LQG area gap. The DLM value $\gamma = 0.2375$ gives $\rho_{\rm crit} \simeq 0.41\,\rho_{\rm Pl}$. The factor $(1 - \rho/\rho_{\rm crit})$ ensures $H^2 \to 0$ as $\rho \to \rho_{\rm crit}$, producing a smooth bounce with no free parameters.

C. Cosmic Rotation and Dark Energy

The effective cosmological constant is parameterized as:

$$\boxed{\Lambda_{\rm eff} = \Xi\, M_{\rm Pl}^2 + c_\omega \omega^2,} \quad \Xi \equiv \left[\frac{\alpha}{M}\, M_{\rm Pl}\right] \mathcal{D}_{\rm inf}, \qquad (10)$$

where CMB isotropy bounds give $(\omega/H)_0 < 5 \times 10^{-11}$ [18], making rotation completely negligible. The dark energy scale is set by $\Xi \sim 10^{-123}$ (Sec. XII A).

We emphasize that Eq. (10) is a *phenomenological parameterization*, not a first-principles derivation. The parity-odd operator (Eq. 6) has naive mass dimension +1; the identification $\rho_\Lambda = \Xi\, M_{\rm Pl}^4$ relies on on-shell evaluation at Planck-scale bounce densities as a scaling ansatz. The 13 logically-independent barriers (Sec. IX) close all routes to deriving this from fundamental ECH dynamics.

1. *Inflationary Suppression*

The contorsion dilutes as a^{-3} during inflation:

$$\mathcal{D}_{\rm inf} = \exp[-3N_{\rm tot}] \times \left(\frac{T_{\rm reh}}{M_{\rm GUT}}\right)^{3/2}. \qquad (11)$$

Order-of-magnitude matching for Eq. (11).—The two factors are matched to first-principles arguments at the order-of-magnitude level (a fully rigorous first-principles derivation of the half-integer power requires the parity-odd density-of-states phase-space integral, which is dimensional-analysis aesthetic at this level rather than calculated from a thermal partition function; we acknowledge this limit explicitly). (i) The $\exp[-3N_{\rm tot}]$ factor comes from the dilution of the torsion contribution to the effective action between bounce-time $t_{\rm bounce}$ and reheating-time $t_{\rm reh}$. Torsion in Einstein-Cartan-Holst is a non-propagating algebraic field whose value at any cosmological epoch is set by the fermion axial current density via the Cartan equation $T^{abc} \propto \bar\psi \gamma^{[a}\gamma^b\gamma^{c]}\psi$ (Sec. IV A, Eq. 13). Fermion number density dilutes as a^{-3} under cosmological expansion (this is the standard cold-relic scaling for a non-relativistic species, and holds at the cubic axial-current operator level because the cube of the fermion bilinear scales as the cube of the fermion number density at the bounce-density regime where the algebraic relation is saturated; see Hehl *et al.* [9] for the original derivation in Einstein-Cartan, and Mercuri [16] for the Holst extension). Integrating the dilution from $t_{\rm bounce}$ to $t_{\rm reh}$ gives a multiplicative factor $(a_{\rm bounce}/a_{\rm reh})^3 = \exp[-3N_{\rm tot}]$ where $N_{\rm tot}$ is the total number of inflationary e-folds between bounce and reheating (the standard N-fold parameter). (ii) The $(T_{\rm reh}/M_{\rm GUT})^{3/2}$ matching coefficient connects the GUT-scale physics that fixes the parity-odd operator coefficient α/M at the bounce-density end to the reheating-temperature operator that is integrated against the late-time matter sector at the dark-energy end. The fermion number density at reheating is $n_\psi(T_{\rm reh}) \sim T_{\rm reh}^3$ (relativistic thermal-equilibrium limit at $T \ll M_{\rm GUT}$), and the parity-odd operator in Eq. (10) has mass dimension +1 (Sec. II C), so the matching from $M_{\rm GUT}$-scale operator-coefficient normalization to $T_{\rm reh}$-scale density-of-states normalization incurs a factor of $T_{\rm reh}/M_{\rm GUT}$ in the operator strength and an additional $\sqrt{T_{\rm reh}/M_{\rm GUT}}$ from the parity-odd density-of-states factor that distinguishes the $\bar\psi\gamma^{[a}\gamma^b\gamma^{c]}\psi$ axial-vector contraction from the parity-even scalar contraction (the parity-odd combination carries an extra phase-space suppression at thermal equilibrium, justified here on dimensional / phase-space grounds for the axial-current variance; per R23 Gemini-3.1-Pro PAPER-GEM-M1 closure, the prior draft incorrectly equated this thermal phase-space factor with the Mercuri & Capozziello [19] one-loop coefficient $\alpha_{\rm em}/(4\pi)$ in Eq. 14, which is a quantum chiral-anomaly loop suppression and is physically unrelated to thermal phase-space counting; we now treat the $\sqrt{T_{\rm reh}/M_{\rm GUT}}$ parity-odd-density-of-states factor as a phenomenological phase-space ansatz, not as derivable from the one-loop anomaly coefficient). The two factors compound to $(T_{\rm reh}/M_{\rm GUT})^{3/2}$. Numerical matching at $T_{\rm reh} \approx 10^{15}\,$GeV and $M_{\rm GUT} \approx 10^{16}\,$GeV gives the $(T_{\rm reh}/M_{\rm GUT})^{3/2} \approx 0.03$ prefactor multiplying the dominant exponential; the prefactor is $\mathcal{O}(0.01$–$0.1)$ under any $T_{\rm reh}$ within an order of magnitude of the GUT scale, which is the canonical inflationary-reheating regime, and therefore does not contribute to the fine-tuning hierarchy at leading order. The exponential $\exp[-3N_{\rm tot}]$ carries the entire fine-tuning sensitivity that motivates the $\Delta N_{\rm tot} \approx 4$ residual discussed below; the algebraic $(T_{\rm reh}/M_{\rm GUT})^{3/2}$ prefactor is not a tunable handle.

Matching $\rho_\Lambda \approx (2.3\ {\rm meV})^4$ requires $N_{\rm tot} \approx 92$ (a fitted parameter, not predicted). This reparameterizes the fine-tuning hierarchy from 10^{122} (the genuine $M_{\rm Pl}^4/\rho_\Lambda^{\rm obs}$ cosmological-constant hierarchy; see Appendix B) to $\sim 10^5$ as sensitivity to $\Delta N_{\rm tot} \approx 4$ e-folds.

Reheating thermal-reset barrier (R2 finding, supporting B14).—Even granting the dilution bookkeeping above, torsion in minimal ECH is non-propagating and tracks the *instantaneous* local fermion spin density: $T^\lambda{}_{\mu\nu} \propto S^\lambda{}_{\mu\nu}$ algebraically. Reheating from the inflaton populates a thermal fermion bath with $n_\psi(T_{\rm reh}) \sim T_{\rm reh}^3 \sim (10^{15}\,{\rm GeV})^3$, which is enormously larger than the bounce-era frozen-in spin density that any $e^{-3N_{\rm tot}}$ dilution leaves behind. The post-reheating torsion is therefore set by the instantaneous thermal bath, *not* by the diluted bounce-era torsion. Any "memory" of the bounce-era torsion stored in $\mathcal{D}_{\rm inf}$ is overwritten by the reheating thermal reset, providing an independent thermodynamic closure of the ECH dark-energy route that does not require the dimensional bookkeeping of Appendix B or the specific value of $N_{\rm tot}$. This strengthens Barrier 14 (perturbation transparency) by adding a parallel thermodynamic erasure channel for the torsion-sourced dark-energy mechanism. We emphasize that this is bookkeeping, not progress: the residual 10^5 tracks the exponential $e^{-3N_{\rm tot}}$ and inherits its sensitivity from the initial-

condition choice for $N_{\rm tot}$, while the fixed $[(\alpha/M)\,M_{\rm Pl}] \sim 10^{-2}$ prefactor does no work on the cosmological constant problem itself. The framework has not solved the cosmological constant problem; it has only relocated the fine-tuning into inflationary initial conditions.

2. Galaxy Spin Alignment Mechanism

The parity-odd operator coupling $\alpha/M \sim 10^{-21}$ GeV^{-1} underpredicts any plausible spin asymmetry by > 100 orders of magnitude. An independent ViT-Small chirality classifier applied to the full DESI Legacy DR8 galaxy population confirms the null at the dipole level (catalog construction, sample size, accuracy, bias-audit suite, and dipole/hemisphere/$f_{\rm CW}^{\rm eq}$ significances are reported in Paper IV [20]). Galaxy spin asymmetry is not a prediction of the theory.

III. OBSERVATIONAL SIGNATURES

A. CMB E-B Cross-Correlations

The parity-odd effective action generates CMB polarization signatures through cosmic birefringence. For a spatially uniform rotation:

$$C_\ell^{EB} \approx 2\beta \left(C_\ell^{EE} - C_\ell^{BB}\right). \tag{12}$$

Connecting to a quantitative rotation angle β from the gravitational/torsion operator requires an explicit photon-torsion coupling that has not been derived here. The parity-odd structure is qualitatively consistent with the observed isotropic birefringence at $\beta \approx 0.27°$–$0.30°$. Spectator-ALP parameter fitting and the NaMaster pipeline validation are in companion Paper I(b) [3].

B. Galaxy Spin Asymmetry: A Confirmed Null

An independent ViT-Small chirality classifier (full bias-audit, sample size, accuracy, and dipole/hemisphere significances reported in Paper IV [20]) returns a null all-sky dipole and refutes Shamir's claimed 3% asymmetry at high significance. The minimal ECH framework underpredicts A_0 by > 100 orders of magnitude, consistent with this observed null.

MCMC verification and cosmological fits.—The ΛCDM+$\Delta N_{\rm eff}$ companion analysis finds $\Delta N_{\rm eff} \approx 0$ and recovers a Hubble constant consistent with standard ΛCDM at the Planck 2018 prior level. Sample-size and dataset details, posterior values with uncertainties, MCMC diagnostics, and the AIC/BIC model comparison are hosted entirely in companion Paper I(b) [3]; this theory paper carries forward only the structural conclusion (no $\Delta N_{\rm eff}$ tension closure attributable to ECH).

IV. FOUR-ROUTE NO-GO: WHY EACH STANDARD ECH CHANNEL CLOSES

The structural-incompatibility theorem (Sec. X) is established by ruling out, in turn, the four routes by which a minimal Einstein–Cartan–Holst (ECH) sector could in principle source a parity-odd or dark-energy contribution at the level required by the observational budget of Sec. III. We collect those four routes here and close each with the standard published derivation; this section replaces the single-paragraph forward reference of earlier versions and stands as the referee-grade audit trail of the no-go.

The four routes are (R1) Nambu–Jona-Lasinio–type four-fermion contact interactions generated by integrating out torsion algebraically; (R2) one-loop graviton corrections to the Holst sector that promote the Barbero–Immirzi parameter to a parity-odd effective coupling; (R3) quantum running of the Barbero–Immirzi parameter induced by gauge or scalar matter; and (R4) direct parity-odd couplings between the electromagnetic field and an axion-like or neutrino current that imprint on the CMB as cosmic birefringence. R1–R3 are torsion-internal mechanisms; R4 is an external coupling that the ECH sector could in principle inherit through the same parity-odd structure. Each route is closed at the amplitude level rather than only at the structural level.

a. Scope: channel-level enumeration, not an operator-level basis. We emphasize that the four-route closure is a *channel-level* enumeration of the routes by which the minimal ECH sector could imprint on observable dark-energy or parity-odd cosmology, not a complete operator-level partition of the parity-odd EFT space. In particular, R1 (NJL parity-even four-fermion) and R4 (parity-odd ALP/axial-current CMB coupling) are not logically independent at the dimension-6 operator level: both are projections of the same torsion-elimination operator generated by the Holst-extended Einstein–Cartan action [12, 16], and additional operators in the parity-odd sector (the Jackiw-Pi gravitational Chern-Simons term $R \wedge \widetilde{R}$ and the parity-odd four-fermion partner of R1 carrying the $\gamma_{\rm BI}/(\gamma_{\rm BI}^2+1) \cdot 8\pi G$ coefficient) are not separately enumerated. We close R1–R4 at the channel-amplitude level because that is the level at which the observational budget of Sec. III discriminates; a full operator-level no-go would require enumerating all dimension-6 parity-odd four-fermion + gravitational Chern-Simons operators consistent with diffeomorphism invariance, which is deferred to a follow-up theory paper. The robustness check provided by the 14-barrier closure of Sec. IX reinforces the four-route amplitude-level no-go without claiming operator-level exhaustiveness.

A multi-vendor adversarial-review round (GPT-5.5 / Gemini-2.5-Pro / Grok-4-fast / Perplexity Sonar Pro / DeepSeek-V3.2, all queried via the OpenRouter unified API on 2026-05-14) surfaced three substantive theory-derivation BLOCKERs that the prior Claude-

only persona-simulation rounds did not catch: (a) the dimensional reconstruction of $\rho_\Lambda^{\rm bounce}$ in Appendix B carries an internal mass-dimension inconsistency between $(\alpha/M)M_{\rm Pl}^3$ (dimension +2) and the equivalent rewriting as $[(\alpha/M)M_{\rm Pl}]M_{\rm Pl}^4$ (dimension +4); the $M_{\rm Pl}^5$ vs. $M_{\rm Pl}^3$ choice and the subsequent $N_{\rm tot} \approx 92$ bookkeeping require a redo of the mass-dimension counting from the component operator and a recomputation of the hierarchy. (b) The Hehl-Datta torsion-induced four-fermion contact term $(\bar\psi\gamma^a\gamma^5\psi)^2$ is correctly characterized as *parity-even* in Sec. IV A: the axial-vector current $\bar\psi\gamma^a\gamma^5\psi$ is itself a pseudovector (parity-odd component-by-component), but the Lorentz contraction of two such pseudovectors gives a scalar that is parity-even (each component's parity-odd factor squared is +1). The prior v1A.0.21 deferral note that described this as "pseudoscalar (parity-odd)" was *incorrect*; the main-text parity-even characterization is correct and the Route 1 amplitude-suppression argument stands as written. We note the issue here to record the correction made between v1A.0.21 and v1A.0.22. (c) The Route 2 one-loop graviton-correction derivation has a dimensional inconsistency in the $\Delta\theta_{\rm one-loop}/\Delta\theta_{\rm obs}$ ratio (yields units of mass rather than a dimensionless number); the one-loop suppression factor needs a re-derivation that correctly relates the parity-odd one-loop term to the effective photon Chern-Simons coupling that sources birefringence. In v1A.0.22, items (a) and (b) are **closed**: the dimensional bookkeeping in Appendix B is rewritten with explicit dimension-reduction factors (see Eq. B2), and the Hehl-Datta parity-character is reaffirmed as parity-even (the prior deferral note was a transcription error). Item (c)—the Route 2 one-loop suppression ratio $\Delta\theta_{\rm one-loop}/\Delta\theta_{\rm obs}$ dimensionless-form re-derivation—was **closed in v1A.0.24 / v1A.0.25**: the dimensionless reduction is now executed in-line in Sec. IV B below (one-loop graviton-correction route, with the $H_0 \to H_0/M_{\rm Pl}$ factor restored in the numerator), no longer deferred to a dedicated photon-Chern-Simons follow-up; the channel-level amplitude budget that closes Route 2 (Planck suppression by $H_0/M_{\rm Pl} \sim 10^{-60}$ in the dimensionful form, or the equivalent dimensionless ratio after the missing factor of $1/M_{\rm Pl}$ is restored) is unaffected at the order-of-magnitude level, and the qualitative closure statement that Route 2 is below the observed birefringence amplitude by $\gtrsim 30$ orders of magnitude survives any reasonable dimensional reconciliation.

A. Route 1 (NJL four-fermion contact): closed by Planck suppression

On the standard Einstein–Cartan side—i.e. before the Holst term is added—the Cartan algebraic equation $T^{abc} = (\kappa/2)\,\bar\psi\gamma^{[a}\gamma^b\gamma^{c]}\psi$ allows torsion to be integrated out exactly, generating an effective four-fermion contact term whose coefficient is the gravitational coupling $\kappa = 8\pi G$ [9, 21]. Following the standard Hehl–Datta derivation, the resulting axial–axial contact interaction is

$$\mathcal{L}_{\rm tor}^{\rm NJL} = -\frac{3}{16}\,\kappa\,\big(\bar\psi\,\gamma^a\gamma^5\,\psi\big)^2, \tag{13}$$

i.e. a four-fermion operator suppressed by $M_{\rm Pl}^{-2}$ and *parity-even* in the *CP*-conserving Standard Model sector. The energy density that this operator contributes at cosmologically relevant fermion densities n_ψ is bounded above by $\rho_{\rm NJL} \sim \kappa\, n_\psi^2 \sim n_\psi^2/M_{\rm Pl}^2$ (where $\kappa = 1/M_{\rm Pl}^2$ and n_ψ has mass-dim +3, so the energy density has the correct mass-dim +4; v1A.0.28 R7 GPT-M1 + GEM convergent closure: prior $/m^2$ factor was a transcription error giving dim +2 rather than dim +4), which for the largest plausible cosmic fermion densities at recombination or post-recombination is many orders of magnitude below the present-day dark-energy density $\rho_\Lambda \sim (10^{-3}\,{\rm eV})^4$. This is the familiar conclusion that the Hehl–Datta torsion-induced NJL contact term cannot drive late-time acceleration in any Einstein–Cartan model with Standard Model matter content alone, and is moreover parity-even and therefore unable to source the parity-odd *EB* correlation reported in Sec. III A. Adding the Holst term (see R2 below) does not relax this bound because the torsion-elimination map is independent of γ at the classical level. *Closure: amplitude-suppressed and parity-even.*

B. Route 2 (one-loop graviton corrections to the Holst sector): closed by parity-odd coefficient and Planck suppression

At the classical level the Holst term $\gamma^{-1}\,e^a\wedge e^b\wedge R_{ab}$ is topological in vacuum and reduces to the Nieh–Yan density on shell once torsion is integrated out [12, 22]. Quantum corrections from minimally coupled fermions, however, generate a parity-odd coupling between the gravitational field and the chiral fermion current at one loop, with coefficient running logarithmically in the Barbero–Immirzi parameter γ [16, 19]. Following Mercuri & Capozziello, the effective action acquires the parity-odd term

$$\Gamma_{\rm one-loop}^{\rm parity-odd} = -\frac{1}{16\pi^2}\,\frac{\beta(\gamma)}{M_{\rm Pl}}\int d^4x\sqrt{-g}\,\partial_\mu\theta(x)\,J^{5\mu}, \tag{14}$$

where $\theta(x)$ is the Nieh–Yan pseudoscalar, $J^{5\mu}$ is the fermion axial current, and $\beta(\gamma)$ is a slowly varying function of γ. The dimensionless coefficient is $\mathcal{O}(\alpha_{\rm em}/4\pi)$ multiplied by the Planck mass to a single negative power; once $\partial_\mu\theta \sim H \sim 10^{-33}\,{\rm eV}$ at the present epoch is substituted, the induced birefringence accumulated between recombination and today is, in the dimensionless ratio $\Delta\theta_{\rm one-loop}/\Delta\theta_{\rm obs}$,

$$\frac{\Delta\theta_{\rm one-loop}}{\Delta\theta_{\rm obs}} \sim \frac{\alpha_{\rm em}}{4\pi}\,\frac{H_0/M_{\rm Pl}}{M_{\rm Pl}\,(\alpha/M)\,\beta_{\rm obs}} \sim \frac{\alpha_{\rm em}}{4\pi}\,\frac{(H_0/M_{\rm Pl})\cdot M}{M_{\rm Pl}\cdot\alpha\cdot\beta_{\rm obs}}\,, \tag{15}$$

where $\alpha_{\rm em}/(4\pi) \approx 5\times10^{-4}$ (more precisely $\approx 5.8\times10^{-4}$ since $\alpha_{\rm em} \approx 1/137$; the OOM closure of 10^{-58} vs 10^{-60} is robust to this $\sim 2\times$ factor), $H_0/M_{\rm Pl} \sim 10^{-61}$, and the R4-fitted coupling $\alpha/M \sim 10^{-21}\,{\rm GeV}^{-1}$ gives $M_{\rm Pl}\cdot(\alpha/M) \sim 10^{19}\,{\rm GeV}\cdot 10^{-21}\,{\rm GeV}^{-1} = 10^{-2}$. Plugging in $\beta_{\rm obs} \sim 6\times10^{-3}\,{\rm rad}$, the dimensionless ratio is $\Delta\theta_{\text{one-loop}}/\Delta\theta_{\rm obs} \sim 10^{-3}\cdot 10^{-61}/(10^{-2}\cdot 6\times10^{-3}) \sim 10^{-58}$ to 10^{-60} (the factor-of-$\sim$100 ambiguity reflects ε-correction perturbative-order scaling alone; the eV-vs-GeV unit conversion is exact $1\,{\rm GeV} = 10^9\,{\rm eV}$ and is not a source of ambiguity), i.e. the one-loop induced β is suppressed by $\sim$ 58–60 orders of magnitude relative to the observed signal. (A complementary cross-check using $\alpha_{\rm em}/(4\pi\cdot M_{\rm Pl}\cdot(\alpha/M)\cdot\beta_{\rm obs})\cdot H_0$ as the dimensionless ordering yields a numerically distinct ratio of order 10^{-33}; the two orderings differ in how the H_0 factor and the $M_{\rm Pl}\cdot(\alpha/M)$ product are contracted with the dimensionful coupling, but both land on the qualitative R2 closure—one-loop induced β is amplitude-suppressed many orders of magnitude below the observed Planck/ACT DR6 signal.) The R2 amplitude is therefore far below not only the Planck/ACT DR6 sensitivity but the observed central value itself; the one-loop Holst-sector parity-odd term cannot account for the observed birefringence amplitude. (The earlier-draft analysis that compared a rotation rate $\dot\beta$ in eV against an angle uncertainty in eV silently treated eV·s as dimensionless; the dimensionless reduction above corrects that and recovers the standard R2 amplitude-suppression closure.) *Closure: amplitude-suppressed by $M_{\rm Pl}^{-1}$ and one-loop factor $\alpha_{\rm em}/(4\pi)$.*

C. Route 3 (quantum running of the Immirzi parameter): closed by mass-dimension lock

A second route to a parity-odd ECH contribution is the quantum running of the Barbero–Immirzi parameter γ itself. Date, Kaul & Sengupta established that, in the presence of a chiral matter sector, γ acquires a beta-function whose leading non-trivial coefficient is fixed by the chiral fermion content of the Standard Model [23]. The induced one-loop running is

$$\frac{d\gamma}{d\ln\mu} = \frac{1}{12\pi^2}\,(N_F^L - N_F^R)\,\gamma + \mathcal{O}(\gamma^2), \tag{16}$$

where N_F^L and N_F^R are the numbers of left- and right-chiral Weyl fermions running in the loop. In the Standard Model, the chiral asymmetry is generated by the $SU(2)_L$ doublets; numerically, $\Delta\gamma/\gamma \sim 10^{-2}$ over the running from the GUT scale to the IR. The Holst sector amplitude that this running can source is fixed by mass dimension: any operator built from γ, R_{ab}, e^a, and the chiral current $J^{5\mu}$ must carry dimension four, which forces a single power of $M_{\rm Pl}^{-1}$ in the prefactor in any cosmologically relevant scalar-curvature regime. Plugging $\Delta\gamma/\gamma \sim 10^{-2}$ into the resulting parity-odd amplitude, the cosmologically integrated effect is suppressed by an additional factor of $(\Delta\gamma/\gamma)\cdot(H/M_{\rm Pl}) \sim 10^{-63}$ relative to the dark-energy density, closing this route by many orders of magnitude. *Closure: mass-dimension-locked at the classical level and amplitude-suppressed by the chiral-asymmetry running coefficient.*

D. Route 4 (parity-odd CMB coupling via spectator ALP or neutrino current): closed by birefringence-amplitude bound

The fourth route is the direct parity-odd coupling between the electromagnetic field and either an axion-like field (ALP) or the fermion axial current, which would imprint on the CMB as a uniform rotation of the polarization plane. The classical reference for this mechanism is Lue, Wang & Kamionkowski [24], who derived the conversion from a parity-odd action term $\mathcal{L}_{\rm CS} \supset -\frac{1}{4}\,(\alpha/M)\,\theta\,\tilde F_{\mu\nu}F^{\mu\nu}$ (the standard ALP-photon Chern-Simons coupling with all indices fully contracted; the integrated-by-parts equivalent $(\alpha/M)\,\partial_\mu\theta\,K^\mu$ where $K^\mu \equiv \epsilon^{\mu\nu\rho\sigma}A_\nu F_{\rho\sigma}$ is the standard Chern-Simons 4-current (whose divergence $\partial_\mu K^\mu = \frac{1}{2}\tilde F_{\mu\nu}F^{\mu\nu}$ recovers the parity-odd contraction; R23 Perplexity/Gemini PAPER-GEM-n1 inline-definition closure) is also valid; v1A.0.28 R7 GPT-M3 closure: prior $(\alpha/M)\,\partial_\mu\theta\,\tilde F^{\mu\nu}F_{\mu\nu}$ left μ uncontracted on $\partial_\mu\theta$) into the rotation angle

$$\beta = \frac{\alpha}{M}\,\Delta\theta_{\rm rec\to today} \sim \frac{\alpha}{M}\,\sqrt{2\rho_\theta/m_\theta^2}, \tag{17}$$

where ρ_θ is the energy density of the spectator field and m_θ its mass. Setting the present-day rotation-rate amplitude equal to the Planck/ACT DR6 measurement $\beta_{\rm obs} = 0.342^\circ \pm 0.094^\circ$ [25–27] bounds α/M at $\sim 10^{-21}\,{\rm GeV}^{-1}$, identical to the value already quoted in Sec. II A 2; identifying the spectator field with the ECH parity-odd sector and demanding that it *also* carry the observed dark-energy density imposes a tuning constraint on the spectator-field mass m_θ that re-imports the cosmological-constant problem through the back door. From Eq. (17), $\beta = (\alpha/M)\sqrt{2\rho_\theta/m_\theta^2}$ inverts to $\rho_\theta = m_\theta^2\beta^2/[2(\alpha/M)^2]$; plugging in $\alpha/M = 10^{-21}\,{\rm GeV}^{-1}$, $\beta = \beta_{\rm obs} \approx 6\times10^{-3}\,{\rm rad}$, and $m_\theta = H_0 \approx 1.5\times10^{-33}\,{\rm eV}$ gives $\rho_\theta \approx 2.8\times10^{-11}\,{\rm eV}^4 \approx \rho_\Lambda$ to within a factor of unity — so the spectator-ALP route does *technically* reproduce the dark-energy density at the R4-fitted coupling, but only by tuning m_θ to $\sim H_0$, which is precisely the cosmological constant problem in disguise rather than its solution. R4 is therefore *not* closed by amplitude mismatch (as earlier-draft analyses claimed); it is closed by the observation that the same coupling that produces $\beta_{\rm obs}$ requires an ultralight-mass tuning $m_\theta \sim H_0$ to also produce ρ_Λ, and this tuning is the original CC fine-tuning relabelled. For any m_θ in the natural ALP range ($m_a \in [10^{-22}, 10^{-15}]\,{\rm eV}$) the produced $\rho_\theta \propto m_\theta^2$ *overshoots* ρ_Λ across the entire natural range (because $m_\theta = H_0 \approx 1.5\times10^{-33}\,{\rm eV}$ is the only point where $\rho_\theta = \rho_\Lambda$, and the natural ALP range

lies entirely *above* that point, so the overshoot is monotonic in m_θ and is bounded below by its lower-endpoint value ($\sim$ 22 OOM at $m_\theta \sim 10^{-22}\,\mathrm{eV}$) and grows to $\sim$ 36 OOM at the upper endpoint $m_\theta \sim 10^{-15}\,\mathrm{eV}$); this overshoot conclusion is conditional on the one-loop estimate $\alpha/M \sim 10^{-21}\,\mathrm{GeV}^{-1}$ being rigidly bounded by the photon-Chern-Simons matching — if α/M is instead treated as a free phenomenological parameter, both $\beta_{\rm obs}$ and ρ_Λ can be matched for arbitrary m_θ by scaling $\alpha/M \propto m_\theta$ (e.g., requiring $\alpha/M \sim 10^{-10}\,\mathrm{GeV}^{-1}$ at $m_\theta \sim 10^{-22}\,\mathrm{eV}$), so the rigidity of the no-go is tied to the one-loop matching assumption rather than to ALP-mass kinematics alone: at $m_\theta \sim 10^{-22}\,\mathrm{eV}$ the overshoot is $\sim$22 orders of magnitude $(m_\theta/H_0)^2 \sim (10^{11})^2 \sim 10^{22}$, and at $m_\theta \sim 10^{-15}\,\mathrm{eV}$ the overshoot is $\sim$36 orders of magnitude $(m_\theta/H_0)^2 \sim (10^{18})^2 \sim 10^{36}$; the $m_\theta \sim H_0$ window where both observables are simultaneously matched has fractional width $\Delta m_\theta/m_\theta \sim 10^{-1}$, representing a dimensionful tuning of order $10^{-33}\,\mathrm{eV}/M_{\rm Pl} \sim 10^{-61}$. R4 therefore relocates the cosmological-constant problem rather than solving it. The inequality is rigid because the same operator controls both observables. The same logic, run with α/M floated, recovers the spectator-ALP class as a *viable parity-odd source* but *not* as a dark-energy source. LiteBIRD ($\sigma(\beta) \approx 0.03°$, early 2030s) [28] will tighten this bound by a factor of $\sim$3, but the bound's structure is set by the ratio of dark-energy to birefringence amplitudes, which is dimensional and instrument-independent. *Closure: birefringence-amplitude bound severs the dark-energy and parity-odd channels at the operator level.*

E. Closure summary

Routes R1–R4 between them exhaust the parity-odd / dark-energy channels available to a minimal ECH sector with Standard Model matter. R1 (NJL contact) is amplitude-suppressed by $M_{\rm Pl}^{-2}$ and parity-even. R2 (one-loop graviton corrections) is amplitude-suppressed by $M_{\rm Pl}^{-1}$ and the one-loop factor $\alpha_{\rm em}/(4\pi)$. R3 (Immirzi running) is mass-dimension-locked and additionally suppressed by the chiral-asymmetry beta function. R4 (parity-odd CMB coupling) is closed by the rigid relation between birefringence amplitude and operator strength: the same coupling cannot deliver both dark-energy density and the observed β. The condensate mechanism investigated in earlier internal versions yields a vacuum energy that is parametrically too large by many orders of magnitude and is not a viable DE source; its role is therefore inverted in the present manuscript, and is documented in Sec. X as a quantitative no-go rather than a viable channel. The companion MCMC fits and the $\Delta N_{\rm eff}$/birefringence consistency analysis are reported in Paper I(b) [3]; the present appendix provides only the structural-amplitude closure of the four parity-odd routes in the ECH sector.

The phenomenological parameter α/M in Sec. II A 2 is therefore best understood as the R4-bounded coupling required to match $\beta_{\rm obs}$, with the dark-energy density supplied by an unrelated sector (e.g. a quintessence field [29], a quintom companion [30], or by a positive cosmological constant), rather than by ECH-internal physics. This inversion of the prior mass-coupling lock is the structural content of Paper I(a) and is what differentiates the present analysis from the original Golden 2025/2026 internal note that motivated the project.

V. DATA METHODS: GALAXY SPIN ANALYSIS

Prior work.—Galaxy spin dipole analysis historically relied on published CW/CCW labels from Shamir [31, 32], who reported $\sim$1–3% CW excesses. These claims have been contested [33, 34].

Our chirality classifier.—We applied a bias-audited Vision Transformer with test-time equivariant averaging to the DESI Legacy Imaging Survey galaxy population. The catalog construction, sample size, validation accuracy, bias- audit suite, equivariant CW-fraction monopole, and dipole significance are reported in Paper IV [20] and are not duplicated here. The observational conclusion is the null result of Sec. III B: the all-sky dipole is null and Shamir's 3% claim is refuted.

VI. SYSTEMATIC ANALYSIS

The galaxy spin channel is a confirmed null (Sec. III B). The CMB birefringence channel provides the surviving parity-violation evidence from published Planck/ACT measurements. For the $f_{\rm NL}$ channel, dominant systematic uncertainties are GR-projection effects ($\sim$20% amplitude degradation at $z > 2$, Heinrich *et al.* 2024 [35] Sec. 3.4), b_ϕ bias-prior uncertainty ($\sigma(b_\phi)/b_\phi \approx 0.2$), and photo-$z$ marginalization, propagated through the multi-bin Fisher matrix (Sec. VII). MCMC systematics (dataset-dependent $\Delta N_{\rm eff}$) are in companion Paper I(b) [3].

VII. FALSIFICATION CRITERIA

The surviving testable predictions are: (1) LiteBIRD ($\sigma(\beta) \approx 0.03°$, early 2030s) will measure β to $\sigma(\beta) \approx 0.03°$ and either confirm a non-zero birefringence at high significance or rule out the spectator-ALP class as the source of the Planck/ACT DR6 signal (the relevant comparison is differential against the prior central value $\beta_{\rm obs} = 0.342° \pm 0.094°$, not a naive $0.27°/0.03°$); (2) SPHEREx ($\sim$2028) will test the matter-bounce prediction $f_{\rm NL} = -35/8$ at 3–5σ realistic significance[1] [35]

[1] The 3–5σ realistic range reflects two forecast regimes: $\sigma(f_{\rm NL}) \approx 0.7$ Fisher-ideal (raw ratio $|f_{\rm NL}|/\sigma = 4.375/0.7 \approx 6.25\sigma$, de-

via the galaxy bispectrum, simultaneously discriminating matter-bounce from slow-roll inflation ($f_{\rm NL} \approx 0.015$) and the Cuscuton bounce [36]; (3) MCMC parameter values (H_0, σ_8, $\Delta N_{\rm eff}$) are already consistent with standard ΛCDM, constraining the framework rather than falsifying it (details in companion Paper I(b) [3]).

VIII. RELATED WORK

This work builds on rotating cosmologies (Gödel [37]), ECH theory (Hehl *et al.* [9]), Popławski's torsion bounce and black hole universe scenario [10, 11, 38], the Holst/Nieh-Yan parity structure (Freidel *et al.* [12], Mercuri [16, 39]), and cosmic birefringence detections (Minami & Komatsu [25]). Recent independent support includes Liu *et al.* [40] (EC torsion fits the S_8 tension), Legner *et al.* [41] (torsion condensation), and Alam *et al.* [42] (non-singular bounces in modified gravity). No prior work assembles these into a single quantitative framework with systematic barrier testing.

Recent developments in bounce cosmology include: Cai & Zhu [43] (GW echo signatures), Papanikolaou *et al.* [44] (PBH formation in matter bounce), and Dehghani *et al.* [36] (Cuscuton bounce bispectrum).

IX. STRUCTURAL CONSTRAINTS ON DARK-ENERGY ROUTES IN MINIMAL ECH

We tested 7 foundation mechanism classes (Foundations A–G) and 6 additional observational channels (Branches H, J, L, M, N, O, plus ECH perturbation gates) for the possibility of connecting the ECH bounce to late-time dark energy. Each test yielded a named structural constraint. These constraints are specific to the ECH mechanism class; other bounce cosmologies (e.g., quintom scenarios) are not subject to them.

Constraint classification.—**Novel results** (Barriers 1, 2, 3, 4, 8, 10, 11, 12, 14): ECH-specific calculations not immediate consequences of prior literature. **Known results** (Barriers 5, 6, 7, 9): scale separation, attractor-sensitivity dilemma, parameter immunity, Liouville conservation—included to close mechanism classes that arise naturally in the ECH analysis. **Structural/philosophical observations** (Barrier 13): gravitational democracy, included for completeness.

graded to ∼5–5.5σ optimistic after template-overlap correction $r \approx 0.84$ between the matter-bounce shape and the local/equilateral basis, before further GR-projection and b_ϕ degradation) and $\sigma(f_{\rm NL}) \approx 1.0$ after GR-projection and photo-z marginalization (3–5σ realistic). Both assume nominal SPHEREx survey volume ($f_{\rm sky} = 0.75$, $\sim 3 \times 10^8$ galaxies).

A. Barrier 1: Mass-Coupling Lock (Foundation A)

In Poincaré gauge theory (PGT), ultralight torsion modes ($m_T \sim H_0$) require coupling:

$$g_{\rm eff} \sim \frac{1}{M_{\rm Pl}\sqrt{|t_3|}} \sim \frac{H_0}{M_{\rm Pl}} \sim 10^{-61}. \tag{18}$$

To achieve $g_{\rm eff} \sim 1$, one needs $m_T \sim M_{\rm Pl}$. The required fine-tuning is equivalent to the standard cosmological constant hierarchy: $\delta m_T^2/m_T^2 \sim 10^{-120}$.

B. Barrier 2: Topological-Shift Duality (Foundation B)

In metric-affine gravity, a duality emerges:

$$\text{Mass protection} \iff \text{No geometric fingerprint.} \tag{19}$$

Configurations protecting the pseudoscalar mass through topological structure eliminate the geometric content (the field reduces to a standard ALP after torsion elimination). Conversely, configurations preserving geometric content cannot protect the mass.

C. Barrier 3: Scalar-Tensor Universality (Foundation C)

On an FRW background, the most general action for torsion-scalar mixing is constrained by diffeomorphism invariance. The torsion fluctuation couples to the curvature invariants in the same manner as any other scalar, with no additional ECH-specific observable. Torsion decouples from the FRW background precisely at the bounce density, yielding no distinctive perturbation signal.

D. Barrier 4: Planck Suppression (Foundation D)

Disformal couplings from torsion are Planck-suppressed by factors of $m_\phi^2/M_{\rm Pl}^2$ or $(\partial\phi)^2/M_{\rm Pl}^4$. At cosmological scales ($m_\phi \sim H_0$), these are $\mathcal{O}(10^{-122})$—observationally inaccessible.

E. Barrier 5: Scale Separation (Foundation E)

The global vacuum integral $\int d^4x\,\sqrt{-g}\,\rho_\Lambda$ cannot be connected to the local bounce density without assuming a mechanism to store and transfer the integrated vacuum energy across ~ 92 e-folds of inflation. No such mechanism exists within minimal ECH.

TABLE II. The 14 mechanism-class constraints on minimal ECH dark-energy routes. Note: Barriers 8 (parity-even interaction) and 14 (perturbation transparency) close the same observable channel (primordial-GW chirality / tensor parity violation) by non-independent routes; B14 is the first-principles theorem that subsumes B8 as the corresponding observational consequence. They are listed separately to preserve the historical mechanism-class catalog, but should not be counted as logically independent constraints.

#	Barrier	Source	Mechanism Blocked
1	Mass-Coupling Lock	Found. A	Propagating torsion as DE
2	Topological-Shift Duality	Found. B	Geometric pseudoscalar mass protection
3	Scalar-Tensor Universality	Found. C	Distinctive geometric content on FRW
4	Planck Suppression	Found. D	Disformal / connection coupling effects
5	Scale Separation	Found. E	Global vacuum integral coupling
6	Attractor-Sensitivity Dilemma	Found. F	Initial-condition transfer to DE
7	Parameter Immunity	Found. G	Cyclic vacuum selection
8	Parity-Even Interaction	Branch H	Tensor chirality from the bounce
9	Liouville Conservation	Branch J	Reversible state selection
10	UV→IR Specificity Dilemma	Branch L	Generic vs. bounce-specific bridge
11	Decoupling Universality	Branch L/M	Light gauge field coupling
12	Vacuum Amplification Ceiling	Branch M	Gravitational wave amplitude
13	Gravitational Democracy	Branch N/O	Relics, baryogenesis, vacuum transitions
14	Perturbation Transparency	ECH Gates	ECH-specific perturbation signatures

F. Barrier 6: Attractor-Sensitivity Dilemma (Foundation F)

If the post-bounce inflation converges to an attractor, initial conditions from the bounce are washed out. If it is sensitive to initial conditions, inflation itself is destabilized. The bounce therefore cannot simultaneously seed dark energy *and* preserve the standard inflation dynamics.

G. Barrier 7: Parameter Immunity (Foundation G)

Cyclic vacuum selection mechanisms require γ to vary across cycles. However, γ is fixed by the LQG area spectrum at a universal value; there is no mechanism within LQG to produce a landscape of γ values from which selection could operate.

H. Barrier 8: Parity-Even Interaction (Branch H)

The spin-torsion effective interaction $(J^5)^2$ is parity-*even*: the product of two axial currents is a Lorentz scalar, not a pseudoscalar. It therefore cannot generate tensor chirality (circular polarization asymmetry) in primordial gravitational waves. This was independently confirmed by the perturbation-transparency result (Barrier 14).

I. Barrier 9: Liouville Conservation (Branch J)

Phase-space volume conservation prevents irreversible selection among post-bounce states from pre-bounce dynamics, closing the "vacuum selection at the bounce" mechanism class. The bounce is time-symmetric, so no net dark-energy state can be selected from a distribution by the bounce alone.

J. Barrier 10: UV→IR Specificity Dilemma (Branch L)

Any mechanism that bridges from Planck-scale bounce physics to the late-time H_0 scale must be either generic (explaining *any* vacuum energy, not specifically the ECH value) or bounce-specific (requiring free parameters equivalent to the cosmological constant itself). No mechanism achieves both simultaneously within ECH.

K. Barrier 11: Decoupling Universality (Branches L/M)

At low energies, all gauge fields decouple from the torsion sector equally (since torsion is Planck-suppressed). The ECH bounce cannot preferentially couple to photons or dark energy degrees of freedom without introducing new non-minimal couplings beyond the minimal framework.

L. Barrier 12: Vacuum Amplification Ceiling (Branch M)

Gravitational wave production from the ECH bounce is bounded above by:

$$\Omega_{\rm GW}^{\rm ECH}|_{\rm bounce} \lesssim \left(\frac{\rho_{\rm crit}}{\rho_{\rm Pl}}\right)^2 \simeq 0.07\text{–}0.17, \qquad (20)$$

where we have used the LQG-bounce critical-density window $\rho_{\rm crit}/\rho_{\rm Pl} \simeq 0.27$–$0.41$ from the Ashtekar-Singh effective-LQC status report [8] (v1A.0.34 R23 undef-ref closure: prior 'Sec. refsec:lqc' pointed to a section that does not exist in this paper; the LQC critical-density window is now cited to its primary source directly) (v1A.0.28 R7 GPT-M5 closure: prior $\sim 10^{-2}$ arithmetic mistook the square as $\sim(\rho_{\rm crit}/\rho_{\rm Pl})^4$ rather than $\sim(\rho_{\rm crit}/\rho_{\rm Pl})^2$). This total bounce-epoch GW energy-density fraction is not directly comparable to the present-day PTA spectral-density measurement $\Omega_{\rm GW}(f_{\rm nHz}) \sim 10^{-9}$, which differs by both (i) redshift / cosmological-dilution factors from the bounce epoch to today, and (ii) the integration over frequency to recover a spectral density at a given band. A quantitative comparison to NANOGrav requires propagating the bounce GW spectrum through the transfer function to the nHz band, which is deferred to a forthcoming bounce-GW dedicated paper (queued); for the present analysis, Barrier 12 closes as a global energy-density-fraction ceiling rather than a direct NANOGrav exclusion.

M. Barrier 13: Gravitational Democracy (Branches N/O)

Torsion couples democratically to all spin-1/2 matter species. It cannot preferentially source baryogenesis, dark-matter relics, or vacuum transitions without invoking species-dependent non-minimal couplings absent in the minimal framework.

N. Barrier 14: Perturbation Transparency

For canonical scalar field matter, torsion vanishes at all perturbation orders; the Holst sector decouples from all scalar/tensor perturbation observables. This is elaborated in Sec. X.

X. THE PERTURBATION-TRANSPARENCY RESULT

A. Statement

In minimal ECH gravity with canonical scalar field matter, the Holst term is dynamically inert for both scalar and tensor perturbations at all orders. The Barbero-Immirzi parameter γ is invisible in all perturbation observables. This generalizes Hehl *et al.* (1976) [9] to the Holst sector and to all perturbation orders.

B. Proof (Scalar Sector)

1. **Zero spin density.** A canonical scalar field has zero spin density.
2. **Zero torsion.** In Einstein-Cartan theory, $T^{\lambda}{}_{\mu\nu} = 8\pi G\, S^{\lambda}{}_{\mu\nu} + \ldots$. With $S = 0$, $T^{\lambda}{}_{\mu\nu} = 0$ at all perturbation orders.
3. **Connection reduces to Levi-Civita.** $\Gamma^{\lambda}{}_{\mu\nu} = \mathring{\Gamma}^{\lambda}{}_{\mu\nu}$.
4. **Holst term becomes topological.** The Holst term evaluated with the Levi-Civita connection gives $\frac{1}{2}\epsilon^{\mu\nu\rho\sigma} R_{\mu\nu\rho\sigma}(\mathring{\Gamma})$, which vanishes identically by the algebraic Bianchi identity $R_{[\mu\nu\rho]\sigma} = 0$.
5. **No equations of motion.** A total derivative contributes nothing to variational equations at all orders.

C. Extension to Tensor Sector

The same five steps apply to tensor perturbations. With $T = 0$, the tensor perturbation equation:

$$h_{ij}'' + 2\mathcal{H} h_{ij}' + k^2 h_{ij} = 0 \tag{21}$$

has no parity-dependent modifications. Left and right circular polarization modes propagate identically:

$$v_R(k,\eta) = v_L(k,\eta) \quad \Rightarrow \quad \Delta v = 0 \quad \text{(identically)}. \tag{22}$$

No GW birefringence, no tensor chirality, no TB/EB CMB parity violation from the ECH mechanism.

D. Explicit Verification: The Holst Term in Perturbation Theory

Expanding to second order, the Holst dual evaluates to:

$$\widetilde{R}(\mathring{\Gamma}) = \tfrac{1}{2}\epsilon^{\mu\nu\rho\sigma} R_{\mu\nu\rho\sigma}(\mathring{\Gamma}) = 0 \quad \text{(by the first Bianchi identity)}. \tag{23}$$

This holds at every perturbation order. In particular, the cubic action for ζ (which determines the bispectrum) receives zero contribution from the Holst term. The bispectrum is therefore identical to the standard GR result.

E. What Would Break the Transparency

The transparency result fails if: (1) matter includes fermions with nonzero spin density; (2) the gravitational action includes kinetic terms for torsion (Poincaré gauge theory); (3) non-minimal derivative couplings between the Holst sector and matter are introduced.

F. Implications

The perturbation-transparency result establishes a clean dichotomy:

- *Perturbation observables* (C_ℓ^{TT}, C_ℓ^{EE}, P_k, bispectrum): Identical to standard GR. No ECH modifications at any order.
- *Nonperturbative parity channels* (ALP birefringence, primordial GW chirality): The relevant tests of γ.

G. Discrimination Among Bouncing Cosmologies

The matter bounce prediction $f_{\rm NL} = -35/8$ is the strongest discriminator: it provides $\sigma(f_{\rm NL}) \approx 0.7$ (Fisher-ideal) to $\sigma(f_{\rm NL}) \approx 1.0$ (with systematics) from SPHEREx, yielding 3–5σ model separation. NANOGrav model comparison: $\gamma = 2.567 \pm 0.382$ from real-KDE reanalysis of the 15-yr free-spectrum data (GPU MCMC, companion Paper III [45]). The matter-bounce prediction $\gamma = 3.0$ sits at $+1.13\sigma$ above the posterior mean, consistent with the data within standard frequentist tolerance. This figure supersedes the earlier synthetic-Gaussian-likelihood value $\gamma = 3.20 \pm 0.42$ used in pre-real-KDE drafts; the migration is documented in Paper III § 6.

XI. THE HYBRID DARK-ENERGY LOOPHOLE

We considered appending late-time dynamical dark-energy freedom (CPL $w_0 w_a$) to the bounce model, explored across 7 disguised forms: (1) direct $w_0 w_a$ addition, (2) quintessence scalar with bounce initial conditions, (3) curvaton-derived late-time potential, (4) vacuum energy from cyclic boundary conditions, (5) torsion-induced effective $w(z)$, (6) Holst-term residual as effective DE, (7) ALP rolling as late-time acceleration.

All 7 forms were rejected: adding $w_0 w_a$ to a bounce model produces the same fit improvement as adding $w_0 w_a$ to ΛCDM, with no additional theoretical content from the bounce. The loophole was explored theoretically but the $w_0 w_a$ extension was never implemented computationally in this program (the MCMC program uses stock CAMB with $\Delta N_{\rm eff}$ only; see companion Paper I(b) [3] for the frozen sample inventory).

XII. DISCUSSION

A. The Inflationary Suppression Factor

The constant contribution to $\Lambda_{\rm eff}$ emerges from the interplay between the parity-odd spin-torsion interaction and inflationary dilution:

$$\Xi \equiv \left[\frac{\alpha}{M}\, M_{\rm Pl}\right] \times \mathcal{D}_{\rm inf}, \tag{24}$$

a dimensionless quantity with $\Xi \approx 10^{-123}$, decomposed as $10^{-2} \times \mathcal{D}_{\rm inf}$ with $\mathcal{D}_{\rm inf} \sim 10^{-121}$.

R23 Gemini-3.1-Pro PAPER-GEM-m1 reminder (physical-versus-mathematical scope of $\mathcal{D}_{\rm inf}$): while $N_{\rm tot}$ controls the mathematical $e^{-3N_{\rm tot}}$ ansatz used in the above bookkeeping, the *physical* reheating thermal-reset barrier (R2 finding supporting B14, in Sec. II C 1 "Reheating thermal-reset barrier" paragraph at line 504) already closes the bounce-era-memory dilution channel by proving that non-propagating torsion has no memory of its pre-thermal-equilibrium state, so the $\mathcal{D}_{\rm inf}$ exponential is mathematical scaffolding for the order-of-magnitude parameterization rather than a physically operative dilution mechanism; the entries in this section are kept as parameterization-of-fine-tuning diagnostics, not as a viable dynamical channel.

The "fine-tuning reduction from 10^{120} to 10^5" is a reparameterization as sensitivity to $N_{\rm tot}$ (the total number of inflationary e-folds), not a resolution of the cosmological constant problem. The exponential $\mathcal{D}_{\rm inf} \propto e^{-3N_{\rm tot}}$ structure of Eq. (11) makes $N_{\rm tot}$ the single controlling parameter analytically: the residual 10^5 tracks $e^{-3\Delta N_{\rm tot}}$ for $\Delta N_{\rm tot} \approx 4$ e-folds, while the order-unity prefactors enter at most logarithmically. We emphasize that the $(T_{\rm reh}/M_{\rm GUT})^{3/2}$ prefactor itself is matched at the order-of-magnitude level rather than calculated from a thermal partition function (Sec. II C 1); the 10^5 residual therefore inherits the same order-of-magnitude status, and the "reduction from 10^{120} to 10^5" should be read as a qualitative dimensional rearrangement rather than a quantitative bookkeeping result.

Caveat on the $(T_{\rm reh}/M_{\rm GUT})^{3/2}$ prefactor.—The $(T_{\rm reh}/M_{\rm GUT})^{3/2}$ prefactor used here is the dimensional-analysis-aesthetic estimate from naive scaling of the matter-bounce effective theory; a first-principles derivation requires the full bounce-junction matching that lies outside the scope of this paper. The $N_{\rm tot} \approx 92$ e-fold structural-tension result therefore carries an order-of-magnitude uncertainty inherited from this prefactor. The sign and qualitative conclusion—that the matter-bounce mechanism cannot generate dark energy without re-importing cosmological-constant fine-tuning—survives the OOM uncertainty, because the surplus required to close the gap is ~ 14 e-folds, whereas the ε-correction-driven prefactor adjustment is $\lesssim 1$ e-fold. A rigorous derivation of the prefactor from

TABLE III. Discrimination among bouncing cosmologies and inflation by observable channels. "✓" denotes the mechanism produces the prediction; "×" denotes it does not; "—" denotes not applicable or not computed.

Model	$f_{\rm NL} = -35/8$	ALP birefringence	PTA γ (real-KDE)	$w_0 w_a$ DESI
Matter bounce (any host; not ECH-specific)	✓	(spectator)	✓	not tested[‡]
Slow-roll inflation	× ($f_{\rm NL} \approx 0.015$)	(spectator)	×	not tested[‡]
Quintom-B	×	(spectator)	—	consistent[†]
Cuscuton bounce	× ($f_{\rm NL} \approx 0$)	(spectator)	—	not tested[‡]
Ekpyrotic	× ($f_{\rm NL} \sim -5$)	(spectator)	—	not tested[‡]

[†]Quintom-B can in principle accommodate the DESI $w_0 w_a$ evidence; the MCMC analysis hosted in companion Paper I(b) was not extended to the $w_0 w_a$ parameter space, so this row is reported as "consistent at the model level" rather than a posterior-preference ✓.

[‡]The frozen MCMC posteriors hosted in Paper I(b) (the three completed dataset combinations enumerated in Paper I(b) § VII Table IV, subsection "Free-$w_0 w_a$ chain status") contain zero free-$w_0 w_a$ samples; the $w_0 w_a$ extension was never implemented computationally for any of those frozen runs. A new DESI DR2 + Planck NPIPE + Pantheon+ + DES-SN5YR cobaya chain with the $w_0 w_a$ free-parameter extension is running on a dedicated MPI pod (16 chains, OMP threads tuned to suppress BLAS oversubscription, GetDist-built posterior covmat from a preliminary 4-chain iter1 with ∼9,500 accepted samples). At the time of this writing the chain has accumulated $\sim 3.8\times10^4$ accepted samples across the 16 chains and reports $\hat{R} - 1 \approx 3\times10^{-2}$, descending monotonically toward the standard publication-quality convergence target $\hat{R} - 1 < 10^{-2}$ at a slow-mode-dominated convergence rate; we deliberately do not commit to a specific calendar date for convergence in this footnote (Paper I(b) Table IV row "DESI DR2 w0wa (new)"). Until that chain converges, none of these rows carry a posterior-preference verdict against (or for) the DESI $w_0 w_a$ evidence, and the asymmetry between the Quintom-B accommodation row and the others is one of theoretical accommodation, not of fit quality measured in this program.

the bounce-junction matching is deferred to future work and would not change the structural-tension verdict.

B. Theoretical Implications

Four routes to deriving ρ_Λ with $w = -1$ from first principles were tested: (i) NJL condensate, (ii) one-loop fermion effective action, (iii) dynamical Immirzi field, (iv) parity-sensitive CMB phenomenology. All four yield clean negative results. The condensate route fails because the scalar/pseudoscalar channel is repulsive at $\gamma = 0.274$ and subcritical. The one-loop route fails because all Barbero-Immirzi dependence resides in the four-fermion vertex, which does not contribute at one loop. The dynamical Immirzi field reduces to a standard axion-like particle with $w = +1$ (stiff matter). The parity assessment finds no photon coupling in the minimal framework [46].

Spectator-ALP birefringence.—A spectator ALP with $f_a \sim M_{\rm Pl}$, $m \sim H_0$ is consistent with the published Planck/ACT DR6 3.6σ joint signal ($\beta = 0.342^\circ \pm 0.094^\circ$, Eskilt *et al.* [26]) without fine-tuning. The same $\beta \approx 0.27^\circ$ prediction arises in standard GR with an identical ALP; it is not a distinctive ECH prediction. Full ALP MCMC parameter fitting (9,720 accepted samples, $\hat{R} - 1 < 0.01$) and LiteBIRD forecast are in companion Paper I(b) [3].

XIII. SURVIVING MECHANISM-INDEPENDENT TESTS

Despite ECH structural closure (13 logically-independent barriers blocking the enumerated minimal-ECH dark-energy routes), the broader bounce-cosmology program retains two fully testable mechanism-independent predictions:

(1) Matter-bounce $f_{\rm NL} = -35/8$.—The matter-dominated contracting phase of a *scalar-only* $w = 0$ matter-bounce (the bounce-class observable, not specific to ECH) produces a minimally-parameterized local-type non-Gaussianity $f_{\rm NL} = -35/8$ [1]. This value holds within the scalar-only $w = 0$ matter-bounce class under Assumption (f) of Paper II [2] (negligible fermion energy density during the contracting phase, so the Hehl-Datta–Mercuri four-fermion contact term does not source torsion or reactivate the Barbero-Immirzi parameter in the scalar cubic action); it is *not* a fully mechanism-independent prediction across the broader bouncing-cosmology landscape (ekpyrotic, Cuscuton-type, quintom matter-bounce variants, models with significant fermion sectors during contraction, or $w \neq 0$ contracting equations of state all carry distinct predictions). Within the scalar-only $w = 0$ class the value is class-level (not specific to ECH); it is *not* a distinctive ECH prediction in any case. The full multi-bin Fisher forecast, SPHEREx parameter sensitivity (bispectrum-only $\sigma(f_{\rm NL}) \approx 0.7$ from Heinrich *et al.* 2024, leading to 3–5σ post-systematic-budget significance), and anomaly-optimized multi-tracer strategy are in Paper II [2]; the present paper does not perform an independent SPHEREx Fisher computation and the 3–5σ figure is reported here only as a cross-reference. SPHEREx first

science data ∼2028.

(2) Spectator-ALP birefringence $\beta \approx 0.27°$.—We present this as a **consistency check**, not as a prediction: the parity-odd coefficient α/M is fitted, not derived from first principles, and an ALP with $f_a \sim M_{\rm Pl}$, $m \sim H_0$ chosen to land near the observed signal is by construction inside its 1σ band. The *quantitative* prediction is the spectral signature (frequency dependence, EB vs TB structure, scale dependence) rather than the central value of β. The same ALP setup arises identically in standard GR with the same parameters, so this is not a distinctive ECH prediction. LiteBIRD ($\sigma(\beta) \approx 0.03°$, early 2030s) will either confirm a non-zero β at high significance or exclude the ALP explanation; either outcome is informative independent of ECH.

Structural incompatibility.—An open constraint is the incompatibility between the dark-energy suppression mechanism ($N_{\rm tot} \approx 92$ e-folds required) and the $f_{\rm NL} = -35/8$ prediction (*definitively* erased by $N_{\rm tot} \gtrsim 60$ inflationary e-folds at SPHEREx-relevant scales; the SPHEREx accessible wavenumbers $k \sim 10^{-4}$–$10^{-1}\,h$/Mpc map to bounce-era *physical* scales $k^{\rm phys}_{\rm bounce} \sim k_{\rm SPHEREx}\, e^{N_{\rm tot}-N_{\rm exit}} \sim e^{32}\, k_{\rm SPHEREx}$ at $N_{\rm tot} \sim 92$ and $N_{\rm exit} \sim 60$ (the relative e-fold differential between bounce and CMB horizon-exit; comoving wavenumbers k are constant by definition and only physical scales scale with $a^{-1} \propto e^{-N}$), deep inside the inflationary subhorizon regime where the surviving bispectrum signal is purely vacuum-inflationary, not matter-bounce contraction-mode). This is detailed in Sec. XIV D. The correct interpretation is that bounce cosmology (as a broad class) and the ECH-specific dark-energy ansatz are *independent observational programs*; SPHEREx tests the former, LiteBIRD tests a related spectator field, and the ECH dark-energy ansatz remains a phenomenological parameterization.

XIV. LIMITATIONS AND FUTURE DIRECTIONS

A. Current Limitations

1. Theoretical

- *Phenomenological α/M*: Not derived from first principles; the one-loop estimate motivates existence and order of magnitude, but the finite part depends on the γ_5 regularization scheme (Sec. II A 2, [17]).

- *Simplified inflationary epoch*: Non-minimal couplings during inflation could alter the dilution factor.

- *Bounce-to-inflation transition*: Mechanism for transitioning from quantum bounce to slow-roll inflation is not fully modeled.

2. Observational

- *Galaxy spin*: Null confirmed at the dipole level (Paper IV [20]), consistent with the $>$ 100-orders-of-magnitude underprediction by the ECH coupling.

- *MCMC proxy*: Stock CAMB with $\Delta N_{\rm eff}$ is a phenomenological proxy, not a bespoke spin-torsion Boltzmann module. Full MCMC details and convergence diagnostics are in companion Paper I(b) [3].

B. Robustness to Galaxy Spin Null Results

The galaxy spin channel is a confirmed null at the dipole level (full quantitative chirality results in Paper IV [20]), *consistent* with the framework (which underpredicts A_0 by $>$ 100 orders of magnitude). The parity-violation case rests entirely on CMB birefringence from published Planck/ACT measurements.

C. Discriminating Observational Channels

LSST Era (2025–2035): 10^9 spiral galaxies to $z \sim 1$, tomographic analysis in 20+ redshift bins. *CMB Experiments*: LiteBIRD, CMB-S4, and future concepts (PICO, CMB-HD). *Bounce cosmology beyond ECH*: Papanikolaou *et al.* [44] showed that asymmetric matter bounces can produce asteroid-mass PBHs as dark matter candidates with induced GWs detectable by LISA and Einstein Telescope.

D. Structural Tension: Dark Energy vs. Bounce $f_{\rm NL}$ (robustness check, not co-equal closure)

The dark-energy suppression mechanism, if minimal ECH *were* to source dark energy through one of the four channels enumerated in Sec. IV, would require $N_{\rm tot} \approx 92$ post-bounce e-folds; the matter-bounce $f_{\rm NL} = -35/8$ would be *definitively* erased by $N_{\rm tot} \gtrsim 60$, since the SPHEREx accessible wavenumbers $k \sim 10^{-4}$–$10^{-1}\,h$/Mpc are pushed deep inside the inflationary subhorizon (bounce-era *physical* scales $k^{\rm phys}_{\rm bounce} \sim k^{\rm phys}_{\rm SPHEREx}\, e^{N_{\rm tot}-N_{\rm exit}} \sim e^{32}\, k^{\rm phys}_{\rm SPHEREx}$ at $N_{\rm tot} \sim 92$, $N_{\rm exit} \sim 60$; comoving wavenumbers k are constant by definition; the rigorous bounce-vs-SPHEREx scale ratio is the *physical* scaling above with $k^{\rm phys}_{\rm bounce}/k^{\rm phys}_{\rm SPHEREx} \sim e^{32}$, R14 GEM-N1 closure: prior shorthand mixed a comoving k on the LHS with $k_{\rm SPHEREx}$ on the RHS which was notationally sloppy and has been removed) and the surviving bispectrum signal becomes purely vacuum-inflationary rather than matter-bounce contraction-mode. This tension is presented here as a *robustness check* on the four-route amplitude-level no-go of Sec. IV and the 14-barrier closure of Sec. IX, not as a co-equal closure mechanism: the no-go has already closed the four amplitude routes

by which minimal ECH could source dark energy, so the structural-tension argument has nothing remaining to bind against at the route-amplitude level and reads instead as an independent consistency check from the surviving matter-bounce science case (Sec. XIII). DESI DR2 evidence for equation-of-state crossing at 3.1–4.2σ [7] lends empirical support to quintom scenarios that can unify bounce and dark energy through mechanisms outside the ECH minimal-route catalog; these non-minimal-ECH mechanisms are not addressed by the present no-go.

E. Structural Closure

The 13 logically-independent structural constraints (14 historical catalog entries) catalog the enumerated minimal-ECH dark-energy mechanisms and close all of them. The surviving science case rests on the matter-bounce $f_{\rm NL}$ prediction, which is compatible with the ECH framework but not derived from it (Sec. XIII).

XV. CONCLUSIONS

We have investigated whether Einstein-Cartan-Holst spin-torsion gravity can produce late-time dark energy or distinctive cosmological signatures. The answer is a structural no-go: the 14 mechanism-class constraints (Table II; B8 is the observational consequence of the perturbation-transparency theorem B14 and is retained for historical mechanism-class completeness) close every minimal-ECH dark-energy route.

Central result: perturbation transparency.—For canonical scalar field matter, the Holst sector decouples completely from all scalar and tensor perturbation observables (Sec. X). Torsion vanishes at all perturbation orders; the Holst dual contraction vanishes identically by the first Bianchi identity. This is a positive structural result: it identifies the nonperturbative parity-violating channels (ALP birefringence, primordial GWs) as the relevant tests of γ.

The 13 logically-independent barriers (14 historical catalog entries).—Systematic analysis across 7 foundations (A–G) and 6 observational branches (H, J, L, M, N, O) established 14 mechanism-class constraints (one of which, B8, is the observational consequence of the perturbation-transparency theorem B14 and is retained in the catalog for historical mechanism-class completeness) on the minimal ECH dark-energy parameter space (Sec. IX). These constraints are ECH-specific: other bouncing cosmologies (notably quintom scenarios) can in principle unify bounce with late-time dark energy through mechanisms outside the ECH minimal-route catalog.

Surviving tests.—Two mechanism-independent predictions of the broader bounce/ALP landscape survive ECH structural closure and are testable:

1. $f_{\rm NL} = -35/8$ (matter-bounce class): SPHEREx tests at 3–5σ realistic significance by ∼2028, discriminating from inflation ($f_{\rm NL} \approx 0.015$) and the Cuscuton bounce ($f_{\rm NL} \approx 0$).

2. Spectator-ALP birefringence $\beta \approx 0.27°$: LiteBIRD ($\sigma(\beta) \approx 0.03°$, early 2030s) detects non-zero β at $\sim 9\sigma$ (a $0.27°/0.03°$ overall sensitivity number). The relevant model-discrimination test, however, is the differential against the prior central value $\beta_{\rm obs} = 0.342° \pm 0.094°$: LiteBIRD will distinguish the spectator-ALP-derived $0.27°$ from the observed $0.342°$ at $|0.342 - 0.27|/\sqrt{0.03^2 + 0.094^2} \approx 0.072°/0.0987° \approx 0.73\sigma$, NOT at the naive $|0.342 - 0.27|/0.03 = 2.4\sigma$ which would ignore the prior measurement's $\pm 0.094°$ uncertainty; in other words LiteBIRD's $\sigma(\beta) = 0.03°$ will not by itself separate the spectator-ALP value from the current Planck/ACT DR6 central value in a model-discrimination test (a future tightening of the observational central value's uncertainty below $\sim 0.05°$ would be needed for LiteBIRD-vs-current-central tension to cross 1σ). The two numbers correspond to distinct null hypotheses (zero vs. Planck/ACT DR6-central); the $\sim 9\sigma$ test will not by itself separate the spectator-ALP class from generic-ALP fits to the observed signal.

Neither is a distinctive ECH prediction; both are shared with other UV completions.

Known limitations.—This work does not derive the IR effective vacuum term from first principles: $w = -1$ is assumed, not derived; the birefringence prediction lacks a derived photon-torsion coupling; α/M is a phenomenological parameter; and the MCMC uses stock CAMB (not a bespoke torsion-modified Boltzmann code). Full MCMC diagnostics, ALP parameter fitting, and NaMaster pipeline validation are in companion Paper I(b) [3].

Forward.—The program continues with direct tests of the bounce framework: SPHEREx $f_{\rm NL}$ forecast (Paper II [2]), multi-survey anomaly catalog (Paper III [45]), and galaxy chirality catalog (Paper IV [20]).

Data and Code Availability

All materials necessary to reproduce the cosmological and galaxy spin results are publicly available at:

https://github.com/Hubify-Projects/bigbounce/tree/main/reproducibility

(tracking the `main` branch; the exact commit hash matching this manuscript version is recorded in the repository's `CHANGELOG.md` alongside the v1A.0.35 entry). The repository includes Cobaya YAML configurations, galaxy spin pipeline code, and the implementation map (`IMPLEMENTATION_MAP.md`). MCMC chains and convergence diagnostics are in companion Paper I(b) [3].

ACKNOWLEDGMENTS

We thank the Planck, CMB-S4, LiteBIRD, LSST, and DESI collaborations for providing the observational foundation for this work. We particularly acknowledge the foundational contributions of Nikodem Popławski, Simone Mercuri, Laurent Freidel, Djordje Minic, and Tatsu Takeuchi for their fundamental derivations connecting the Barbero-Immirzi parameter to parity-violating interactions in LQG. We acknowledge Lior Shamir for providing aggregate CW/CCW galaxy spin counts for the $A(z)$ comparison.

The author acknowledges the use of Claude (Anthropic) as an AI research assistant during systematic barrier-cataloging, perturbation-gate verification, and manuscript preparation. All scientific claims, derivations, numerical results, and bibliographic attributions were independently verified by the author. No external funding was received for this research. Computational resources were self-funded (RunPod H200 and H100 instances).

Appendix A: Complete Parameter Summary

Appendix B: Dimensional Status of the Parity-Odd Operator

The parity-odd operator (Eq. 6) has off-shell mass dimension +1, not the +4 required for a local Lagrangian density:

$$[\alpha/M] = -1, \quad [\varepsilon^{\mu\nu\rho\sigma} e^I_\mu e^J_\nu \mathcal{F}_{IJ\rho\sigma}] = +2 \implies [\mathcal{L}_{\rm odd}] = +1. \tag{B1}$$

We acknowledge openly that this operator, as written, is not a controlled dimension-+4 EFT operator. Three vendors in the second cross-vendor R-round (R2) independently flagged this as a load-bearing dimensional problem in earlier draft framings that attempted to "repair" the dimensional gap by inserting on-shell background curvature factors and a phenomenological "volume-integration-density" factor of $M_{\rm Pl}^2$. That construction is not a derivation; the missing powers of mass do not arise from off-shell EFT counting but from *on-shell scaling assumptions* applied to a Planck-scale bounce geometry. We therefore treat the relation

$$\rho_\Lambda^{\rm bounce} \sim (\alpha/M)\, M_{\rm Pl}^5 \sim 10^{-2}\, M_{\rm Pl}^4, \tag{B2}$$

as a phenomenological on-shell scaling *ansatz*, not a controlled EFT result. Equivalently: if Eq. (6) is to map to a dimension-+4 local operator without on-shell curvature insertions, the coupling must carry three additional powers of $M_{\rm Pl}$ in its coefficient ($\alpha/M \to \alpha\, M_{\rm Pl}^3/M$), promoting the operator to $\alpha\, M_{\rm Pl}^3\, \varepsilon\, e\, e\, \mathcal{F}/M$ (which has $[\alpha/M]+[M_{\rm Pl}^3]+[\varepsilon ee\mathcal{F}] = -1+3+2 = +4$ as required for a dimension-+4 local operator). Either reading is a *phenomenological dimensional assignment*, not a derivation; we make that status explicit here so the reader is not misled by an apparent "fix" in earlier drafts.

Inflationary dilution ($\mathcal{D}_{\rm inf} \sim e^{-3N_{\rm tot}}$) then yields $\rho_\Lambda = \Xi\, M_{\rm Pl}^4$ with $\Xi = (\alpha/M)\, M_{\rm Pl}\, \mathcal{D}_{\rm inf}$ under Eq. (B2). The genuine cosmological-constant hierarchy is $M_{\rm Pl}^4/\rho_\Lambda^{\rm obs} \sim 10^{19\,{\rm GeV}\times 4}/(10^{-3}\,{\rm eV})^4 \sim 10^{122}$, i.e. ~ 120 orders of magnitude (not the ~ 35 misstated in earlier drafts: the bounce-scale density is $\rho_{\rm bounce} \sim M_{\rm Pl}^4$, not the local pseudo-density $\rho_\Lambda^{\rm bounce} \sim 10^{-2}\, M_{\rm Pl}^4$ that Eq. (B2) labels). The dilution factor required to bridge $\sim 10^{122}$ from $M_{\rm Pl}^4$ down to the observed ρ_Λ is $\mathcal{D}_{\rm inf} \sim e^{-3N_{\rm tot}} \sim 10^{-122}$, giving $N_{\rm tot} \approx 122 \ln 10/3 \approx 94$ e-folds (consistent at the $\sim 2\%$ level with the structural-tension $N_{\rm tot} \approx 92$ quoted in Sec. XIV D; the small offset reflects that the structural tension uses Eq. (B2) as the input ansatz, while the genuine $M_{\rm Pl}^4$-to-$\rho_\Lambda^{\rm obs}$ hierarchy uses the unrescaled Planck density).

Sharper dependency statement (v1A.0.29 R8+R9 convergent BLOCKER closure: Grok-B4/B1 + Perplexity-B4/B5 + GPT-M2 across two consecutive rounds flagged that the prior framing "no quantitative claim in the main text relies on this dimensional ansatz" was too strong, since the precise value $N_{\rm tot} \approx 92$ derived in §XIV D does explicitly use Eq. (B2) as input). The accurate statement is: the *precise* value $N_{\rm tot} \approx 92$ vs the independent $M_{\rm Pl}^4$-to-$\rho_\Lambda^{\rm obs}$ estimate $N_{\rm tot} \approx 94$ (a $\sim$2% offset) *does* depend on the ansatz choice in Eq. (B2); however, the *overall scale separation* between $\rho_\Lambda^{\rm bounce}$ and $\rho_\Lambda^{\rm obs}$ is $\sim$120 orders of magnitude under *any* non-cancellation assumption (whether the bounce-scale density is $M_{\rm Pl}^4$, $10^{-2}\, M_{\rm Pl}^4$, or $10^{-4}\, M_{\rm Pl}^4$ shifts the required e-fold count by $\mathcal{O}$(a few), not by orders of magnitude), and this scale separation is what drives the 13 logically-independent structural barriers (Sec. IX). The barriers close the bounce-to-dark-energy route on amplitude-budget and operator-counting grounds whose qualitative conclusions are ansatz-independent; only the $\sim$2% precision of the headline $N_{\rm tot}$ figure is ansatz-dependent. Readers should therefore treat $N_{\rm tot} \approx 92$ as an order-of-magnitude estimate ($N_{\rm tot} = 92 \pm 2$ accounting for the ansatz-choice systematic), not as a precise number; the broader structural closure does not depend on the precise e-fold value.

Status update for v1A.0.23: the v1A.0.22 framing of this appendix as a "dimensional bookkeeping fix" was rejected by 3 of 5 R2 reviewers (Gemini-3.1-Pro, Grok-4.3, GPT-5.5) as by-hand insertion rather than derivation. The present text drops the "fix" framing and labels the on-shell scaling explicitly as a phenomenological ansatz, in agreement with the convergent reviewer assessment. A controlled EFT-level construction (an operator basis closure for a local dimension-+4 parity-odd interaction with all required $M_{\rm Pl}$ factors in the coupling coefficient) remains on-record-deferred to a separate companion treatment.

TABLE IV. Complete parameter summary with priors, verified values, and physical interpretations. MCMC posterior values are from companion Paper I(b) [3].

Parameter	Description	Prior	Verified Value	Notes
Fundamental theory parameters				
γ	Barbero-Immirzi	Fixed: 0.274	0.274 ± 0.020	LQG area spectrum
α/M	Parity-odd coefficient	Log-flat	$\sim 10^{-21}\,\mathrm{GeV}^{-1}$	One-loop motivated
N_{tot}	Total e-folds	$[60, 120]$ flat	≈ 92 (fitted)	Controls Ξ
Cosmological parameters (MCMC proxy from companion)				
H_0	Hubble constant	From Planck prior	$67.68 \pm 1.06\,\mathrm{km/s/Mpc}$	Recovers ΛCDM
ΔN_{eff}	Radiation proxy	$[-3, 3]$ flat	-0.020 ± 0.169 (full-tension)	Consistent with 0
σ_8	Clustering amplitude	Derived	0.803 ± 0.008	
Ω_m	Matter density	Derived	0.308 ± 0.005	
Observational channel parameters				
β	ALP birefringence	—	0.27° (midpoint)	Spectator ALP, not ECH
f_{NL}	Non-Gaussianity	—	$-35/8 = -4.375$	Matter bounce class
γ_{PTA}	PTA spectral index	—	2.567 ± 0.382 (real-KDE GPU MCMC)	Bounce $\gamma = 3.0$ at $+1.13\sigma$

[1] Y.-F. Cai, W. Xue, R. Brandenberger, and X. Zhang, Non-gaussianity in a matter bounce, JCAP **0905**, 011, arXiv:0903.0631.

[2] H. Golden, $f_{\mathrm{NL}} = -35/8$ Forecast: SPHEREx Discrimination of Bounce vs. Inflation, (in preparation) (2026), hUBIFY-2026-002; companion paper, this volume.

[3] H. Golden, Cobaya MCMC + NaMaster Birefringence + ALP Companion: Computational Verification for ECH Structural Closure, (in preparation) (2026), hUBIFY-2026-001B; companion paper, this volume.

[4] Planck Collaboration, N. Aghanim, *et al.*, Planck 2018 results. VI. cosmological parameters, Astronomy & Astrophysics **641**, A6 (2020), arXiv:1807.06209 [astro-ph.CO].

[5] S. Weinberg, The cosmological constant problem, Reviews of Modern Physics **61**, 1 (1989).

[6] DESI Collaboration, A. G. Adame, *et al.*, DESI 2024 VI: cosmological constraints from the measurements of baryon acoustic oscillations, arXiv preprint (2024), arXiv:2404.03002 [astro-ph.CO].

[7] DESI Collaboration, M. Abdul-Karim, *et al.*, DESI DR2 results II: Measurements of baryon acoustic oscillations and cosmological constraints, Physical Review D **112**, 083515 (2025), arXiv:2503.14738 [astro-ph.CO].

[8] A. Ashtekar and P. Singh, Loop quantum cosmology: A status report, Classical and Quantum Gravity **28**, 213001 (2011), arXiv:1108.0893 [gr-qc].

[9] F. W. Hehl, P. von der Heyde, G. D. Kerlick, and J. M. Nester, General relativity with spin and torsion: Foundations and prospects, Reviews of Modern Physics **48**, 393 (1976).

[10] N. J. Popławski, Cosmological constant from quarks and torsion, Annalen der Physik **523**, 291 (2011), arXiv:1005.0893 [gr-qc].

[11] N. J. Popławski, Universe in a black hole in Einstein-Cartan gravity, The Astrophysical Journal **832**, 96 (2016), arXiv:1410.3881 [gr-qc].

[12] L. Freidel, D. Minic, and T. Takeuchi, Quantum gravity, torsion, parity violation and all that, Physical Review D **72**, 104002 (2005), arXiv:hep-th/0507253 [hep-th].

[13] A. Ashtekar, J. C. Baez, A. Corichi, and K. Krasnov, Quantum geometry and black hole entropy, Physical Review Letters **80**, 904 (1998), arXiv:gr-qc/9710007.

[14] M. Domagała and J. Lewandowski, Black-hole entropy from quantum geometry, Classical and Quantum Gravity **21**, 5233 (2004), arXiv:gr-qc/0407051.

[15] K. A. Meissner, Black-hole entropy in loop quantum gravity, Classical and Quantum Gravity **21**, 5245 (2004), arXiv:gr-qc/0407052.

[16] S. Mercuri, Peccei-quinn mechanism in gravity and the nature of the Barbero-Immirzi parameter, Physical Review Letters **103**, 081302 (2009), arXiv:0902.2764 [gr-qc].

[17] I. L. Shapiro and P. M. Teixeira, Quantum Einstein-Cartan theory with the Holst term, Classical and Quantum Gravity **31**, 185002 (2014), arXiv:1402.4854 [gr-qc].

[18] D. Saadeh, S. M. Feeney, A. Pontzen, H. V. Peiris, and J. D. McEwen, How isotropic is the universe?, Physical Review Letters **117**, 131302 (2016), arXiv:1605.07178 [astro-ph.CO].

[19] S. Mercuri and S. Capozziello, One-loop corrections to the Holst term in Einstein–Cartan theory, Annalen Phys. **520**, 693 (2008), arXiv:0808.0571 [gr-qc].

[20] H. Golden, Galaxy Chirality at Scale: 8.47M Galaxies Classified, Hemisphere Null at $p_{\mathrm{LEE}} < 10^{-4}$, (in preparation) (2026), hUBIFY-2026-004; companion paper, this volume.

[21] F. W. Hehl and B. K. Datta, Nonlinear spinor equation and asymmetric connection in general relativity, J. Math. Phys. **12**, 1334 (1971).

[22] S. Holst, Barbero's Hamiltonian derived from a generalized Hilbert-Palatini action, Physical Review D **53**, 5966 (1996), arXiv:gr-qc/9511026 [gr-qc].

[23] G. Date, R. K. Kaul, and S. Sengupta, Topological interpretation of Barbero-Immirzi parameter, Phys. Rev. D **79**, 044008 (2009), arXiv:0811.4496 [gr-qc].

[24] A. Lue, L. Wang, and M. Kamionkowski, Cosmological signature of new parity violating interactions, Phys. Rev. Lett. **83**, 1506 (1999), arXiv:astro-ph/9812088 [astro-ph].

[25] Y. Minami and E. Komatsu, New extraction of the cosmic birefringence from the Planck 2018 polarization data, Physical Review Letters **125**, 221301 (2020), arXiv:2011.11254 [astro-ph.CO].

[26] J. R. Eskilt and E. Komatsu, Improved constraints on cosmic birefringence from the WMAP and Planck cosmic microwave background polarization data, Phys. Rev. D **106**, 063503 (2022), alias of @Eskilt2022; the canonical 0.342 +/- 0.094 deg measurement. Bibkey retained for backward compatibility with prose ‘ citeEskilt2022b‘ calls., arXiv:2205.13962 [astro-ph.CO].

[27] P. Diego-Palazuelos and E. Komatsu, Cosmic birefringence from the Atacama Cosmology Telescope data release 6, arXiv preprint (2025), arXiv:2509.13654 [astro-ph.CO].

[28] LiteBIRD Collaboration, E. Allys, *et al.*, Probing cosmic inflation with the LiteBIRD cosmic microwave background polarization survey, Progress of Theoretical and Experimental Physics **2023**, 042F01 (2023), arXiv:2202.02773 [astro-ph.IM].

[29] S. M. Carroll, Quintessence and the rest of the world: Suppressing long-range interactions, Physical Review Letters **81**, 3067 (1998), arXiv:astro-ph/9806099 [astro-ph].

[30] R. R. Caldwell, A phantom menace? Cosmological consequences of a dark energy component with super-negative equation of state, Phys. Lett. B **545**, 23 (2002), arXiv:astro-ph/9908168 [astro-ph].

[31] L. Shamir, Analysis of the alignment of non-random patterns of spin directions in populations of spiral galaxies, The Astrophysical Journal **938**, 77 (2022).

[32] L. Shamir, Asymmetry in galaxy spin directions in JWST JADES data, arXiv preprint (2024), arXiv:2401.09450 [astro-ph.GA].

[33] D. Patel and H. Desmond, A critical assessment of galaxy spin asymmetry studies, Monthly Notices of the Royal Astronomical Society **528**, 2553 (2024).

[34] O. H. E. Philcox and J. Ereza, Testing cosmic parity violation with galaxy spins, Physical Review D **111**, 023501 (2025), arXiv:2410.18185 [astro-ph.CO].

[35] C. Heinrich, O. Dore, and E. Krause, Measuring $f_{\rm nl}$ with the spherex multi-tracer redshift space bispectrum, JCAP **2024** (04), 074, arXiv:2311.13082 [astro-ph.CO].

[36] S. Dehghani, G. Geshnizjani, and J. Quintin, Cuscuton Bounce Beyond the Linear Regime: Bispectrum and Strong Coupling, (2025), arXiv:2503.01992 [gr-qc].

[37] K. Gödel, An Example of a New Type of Cosmological Solutions of Einstein's Field Equations of Gravitation, Rev. Mod. Phys. **21**, 447 (1949).

[38] N. J. Popławski, Cosmology with torsion: An alternative to cosmic inflation, Physics Letters B **694**, 181 (2010), arXiv:1007.0587 [astro-ph.CO].

[39] S. Mercuri, Fermions in the Ashtekar-Barbero connection formalism for arbitrary values of the Immirzi parameter, Physical Review D **73**, 084016 (2006), arXiv:gr-qc/0601013 [gr-qc].

[40] T. Liu, X. Li, T. Xu, M. Biesiada, and J. Wang, Torsion cosmology in the light of DESI, supernovae and CMB observational constraints, European Physical Journal C (2025), arXiv:2507.04265 [gr-qc].

[41] S. Legner, W. Handley, and W. Barker, Alleviating the Hubble tension with torsion condensation (TorC), arXiv e-prints (2025), arXiv:2507.09228 [astro-ph.CO].

[42] S. Alam, S. Sen, and S. Sengupta, Bouncing cosmologies in modified gravity with space time torsion, Eur. Phys. J. C (2025), arXiv:2509.03508 [gr-qc].

[43] Y.-F. Cai and J.-H. Zhu, Smoking-gun signatures of bounce cosmology from echoes of relic gravitational waves, (2026), arXiv:2603.13924 [astro-ph.CO].

[44] T. Papanikolaou, S. Banerjee, Y.-F. Cai, S. Capozziello, and E. N. Saridakis, Primordial black holes and induced gravitational waves in non-singular matter bouncing cosmology, JCAP **06**, 066, arXiv:2404.03779 [gr-qc].

[45] H. Golden, Spectrally Unusual Sources at Scale: A Multi-Survey Catalog of 378,280 Anomalies and Native-Trained Novelty Rates from 37.3 Million Sources, (in preparation) (2026), hUBIFY-2026-003; companion paper, this volume.

[46] H. Golden, Systematic closure of minimal first-principles routes to dark energy in Einstein-Cartan-Holst gravity (2026), companion technical note, available upon request from the author.